Elsevier Editorial System(tm) for Applied Catalysis B: Environmental

Manuscript Draft

Manuscript Number: APCATB-D-18-04738R1

Title: Correlation preparation parameters/activity for microTiO2 decorated with SilverNPs for NOx photodegradation under LED light

Article Type: VSI: Nov-Mat-Photo-Cat

Keywords: Micro-sized TiO2; LED; AgNPs; NOx degradation

Corresponding Author: Professor Claudia Letizia Letizia Bianchi,

Corresponding Author's Institution: Università degli Studi di Milano

First Author: Giuseppina Cerrato

Order of Authors: Giuseppina Cerrato; Federico Galli; Daria C Boffito; Lorenza Operti; Claudia Letizia Letizia Bianchi

Research Data Related to this Submission

There are no linked research data sets for this submission. The following reason is given:
Data will be made available on request

Dear colleague,
We are setting up a special issue on "Novel Materials for Photocatalytic Applications" to be published in Applied Catalysis B: Environmental (IF=11.69). The thematic areas of the special issue include but not limited to new materials as potential photocatalysts, photocatalysis for self-cleaning and VOC removal, new challenges in photocatalysis, photocatalytic materials for environmental disinfection and decontamination.

As the guest editors of the special issue, we note that you have recently published research related to photocatalytic environmental remediation and have a high quality publication records. Therefore, we would like to invite you to contribute a comprehensive review article or a full research paper for peer-review and possible publication. We believe you would be able to make an excellent contribution on the topic of novel materials for photocatalytic applications for this issue. Please confirm your contribution to the special issue by **September 15, 2018**.

The deadline for manuscript submission is **October 30, 2018**. You may send your manuscript at any time before the deadline. Submitted papers should not have been published previously, nor be under consideration for publication elsewhere. All the manuscripts should follow the format and guidelines of *Applied Catalysis B: Environmental* and should meet the highest scientific quality standards of the journal. Manuscripts should be submitted online through EES system (https://ees.elsevier.com/apcatb/). You must choose **Article Type** as "Special issue-Nov-Mat-Photo-Cat" during the submission process.
All articles will undergo very rigorous peer-review. Please include this "**letter of invitation from the guest editors**" along with the manuscript.

"This Special Issue is dedicated to honor the retirement of Dr. John Kiwi at the Swiss Federal Institute of Technology (Lausanne), a key figure in the topic of photocatalytic materials for the degradation of contaminants of environmental concern." Authors are invited to add this sentence in the acknowledgement of their contributions.

For more information on manuscript preparation and submission, please visit the Instructions for Authors:
https://www.elsevier.com/journals/applied-catalysis-b-environmental/0926-3373/guide-for-authors

We look forward to your response in the hope that it will be positive.
Yours sincerely

Prof. Dr. Dionysios (Dion) D. Dionysiou, Guest editor
Environmental Engineering and Science program, University of Cincinnati
Tel 513-556-0724; Fax 513-556-4162
E-mail: dionysios.d.dionysiou@uc.edu

Prof. Suresh Pillai, Guest editor
Institute of Technology Sligo, Ireland
Tel: +353 71 9305816
Email: Pillai.Suresh@itsligo.ie

Dr. Sami Rtimi, Guest editor
Swiss Federal Institute of Technology (EPFL), Switzerland
Tel: +41216936803
Email: sami.rtimi@epfl.ch

Biography of Dr. John Kiwi
John Kiwi was born in 1940 in Santiago, Chile. He got his PhD from the Oregon State University, Corvallis, OR, USA in the special field of Radiation and Photochemistry in 1971. Then he joined Notre Dame Radiation Laboratory (Notre Dame, Indiana) as research associate. As guest scientist, he visited the Hahn-Meitner-Institute for Nuclear Chemistry (Berlin, Germany). Then, he moved to join the group of Prof. George Porter (Nobel Prize 1967) at the Royal Institution in London, UK. His work focused on light enhanced heterogeneous catalysis. In 1987, he was invited as a guest scientist at the Department of Chemistry at Hebrew University. In 1992, he was tenured as Private-Docent (Lecturer) at the Department of Chemistry at the Swiss Federal Institute of Technology (EPFL, Switzerland) and assign to lead the

course of Physical Chemistry of the Environment. During his career, he published more than 300 papers (H index 65). He has carried out pioneering work in redox catalysis since early 1980s, in the area of heterogeneous catalysis for environmental remediation addressing conventional colloidal, electrochemical and plasma-assisted preparation of catalysts/photocatalysts.

Sami Rtimi (Ph.D.)
Swiss Federal Institute of Technology (EPFL)
Advanced Oxidation Processes Group (GPAO)
EPFL-SB-ISIC-GPAO
1015 Lausanne, Switzerland
https://www.researchgate.net/profile/Sami_Rtimi
https://www.mendeley.com/profiles/sami-rtimi3/
Get green, leave it on the screen !
****

*Response to Reviewers

Manuscript Number: APCATB-D-18-04738

We would like to thank the reviewers for their pertinent comments. Below, we have responded to each in detail in red. All changes in the manuscript are highlighted in yellow.

Reviewer #3:

Reviewers' comments:

(1) The manuscript should be carefully checked for language and grammar.

The manuscript has been fully revised by a native English person

(2) Number all sections and sub-sections.

Numbering has been added.

(3) Avoid use "We" (We observed…., We also modified ….., We then suspended…..,)

The use of the plural first person was reduced.

(4) The abstract is poorly written and presented. Re-write this section as follows; objectives, methodology, results and conclusions.

Following the reviewer indication, the abstract was fully rewritten.

(5) The introduction section is not focused or structured. The entire section was considered TiO2 and its modification, but never mentioned anything on NOx photodegradation. The introduction section should be rewritten.

The Introduction has been shortened for what concerns TiO_2 and its modification and it has been implemented by adding a section addressed to NOx environmental abatement.

(6) Briefly describe the NOx setup used in this work.

A new sentence was added to the manuscript.

(7) Add a process flow diagram (PFD) for the used experimental setup.

We added a scheme of our setup, and we inserted it in the supporting information file.

(8) How the reaction temperature measured and controlled?

The reactor is equipped with a thermocouple that monitors the temperature, while on the outside a fan dispels any heat generated by the lamps (necessary for UVA lamps, but unnecessary for LED, whose energy dispersed by heat is negligible).

(9) The reproducibility of the data and the magnitude of experimental errors are not clearly examined.

The lower detection limit of the Ecotech Serinus 40NOx is 0.4 ppb and its precision is 0.5 %, whichever is the highest. Therefore, we calculated the error on the NOx conversion using the formula for the error propagation and plotted it in the figures. The error resulted smaller than the symbol size. We added this piece of text in the experimental part an the comment on the error bar in Fig 9 and Fig 10 captions

(10) Describe the NOx analysis using Ecotech Serinus 40NOx and also its calibration.

We checked the calibration of the instrument by sending the gas mixture directly from the NOx cylinder to the instrument. The concentration of NOx measured confirmed the one declared by the gas supplier. We add this comment in the experimental part

(11) Results and discussion section:

-NOx degradation: Re-write this section. Present the results first, describe the results, discuss the results, then compare the results with literature.

The session was checked and rewritten according to the indication of the reviewer.

The quality of figure 9 is poor. Re-plot the graph according to the standard of this journal.

We re-prepared the figures 9a and 9b with a resolution of 300 dpi.

Figure 10: The scale of x-axis is not correct. Also, the figure does not show any points on the lines.

We added the points and inserted an axis break to make the scale sound. The caption of the figure was changed accordingly.

-Add the results of the catalyst morphology (BET surface area and pore size distribution).

As mentioned in the manuscript, there is no evidence of modification of the surface area values among the different samples. In all cases, the same amount of silver was deposited on the TiO_2 particles surface.

-Add the kinetics results to understand the reaction mechanism.

The reaction mechanism for NOx photodegradation is well-known and in our case does not change among the different samples.

One reference was added to highlight the mechanism of the reaction.

-Results for the catalyst reusability should be added.

This is an important point that deserves attention. In this case, Ag/TiO_2 is deposited in the form of a thin layer that cannot undergo to a second cycle of photocatalytic testing. We usually add the results regarding the reusability of the material, as we are aware of their importance in defining whether or not the system is active and for how long/how many cycles it remains stable. In this case, the focus of the paper is simply assessing the activity of the material under LED. We have data on its reusability when applied as a stable coating on ceramic tiles.

-The quality of the graphical abstract is very poor.

Graphical abstract was redrawn.

Reviewer #6: The manuscript reports the preparation of Ag decorated samples for the photocatalytic degradation of NOx.
The manuscript contains a phenomenologic description of the materials properties depending on the preparation recipe without any description of the influence of the preparation conditions on the mechanism of particles formation. In this sense the depth of interpretation is by far insufficient to get new insight.
The introduction poorly describes the application for the selected reaction. No discussion is presented to compare the results obtained with the literature, particularly with respect of the photocatalytic reaction.
As already reported in the answers to Reviewer 3, the Introduction has been rewritten for what concerns titania and its modification, as well as it has been implemented by adding a section addressed to NOx environmental abatement.

The concept of doping is inappropriate in this case, being surface deposition of nanoparticles.
We addressed this comment changing “doping” through all the text with “surface decoration/deposition”.

500 ppb is a very small quantity: please report the sensitivity and precision of the analytic instrument for their detection. Error bars should be also added to the conversion pattern to understand the significance of the small variations of conversion there reported.
We addressed the same comment in the query number (9) of Reviewer 3. The instrument detection limit is 0.5 % or 0.4 ppb depending on which is the highest. The variation of conversion is about ±0.7 %.

Does the definition "micrometric" fit a sample with 110 nm average size?
Yes, all particles with a size larger than 100 nm can be ascribed as micrometric and it is an error the use of nanometric that is mandatory for the range 1-100 nm.

NOx degradation: the authors are strongly advised to take samplings in the very first time of the reaction in order to detect significant variation of the concentration of the reactants. The selectivity to different products and the expected reactions should be reported.
NOx photodegradation is a very studied reaction and the mechanism has been reported many times in the literature. In the revised manuscript we enlarged the introduction adding a part on NOx photodegradation and we added two specific references on the reaction pathway.

Also, the redox potentials of the occurring reactions are needed and should be compared with the flat band potentials of the materials used.

Bowering et al already investigated the redox potentials. The paper is now cited as ref 29.

The radiation absorption pattern of the different samples must be discussed with activity results.

The comparison of these results with literature is needed.

A new image was added into the SI and a new sentence is now present in the text.

Some revision is needed:

Abstract: deposit □ deposited

Pg. 4: a several papers □ several papers

p.11: concertation □ concentration

p. 12: can be evidences □ evidenced

All these errors have been corrected.

***List of Three (3) Potential Reviewers**

List of Referees

Prof. Ing. Christos Argirusis
Professor
Laboratory of Inorganic Materials
National Technical University of Athens
School of Chemical Engineering
Athens, GR-157 80
GREECE
Email: amca@chemeng.ntua.gr

Dr. Bernaurdshaw Neppolian
Professor
SRM Research Institute
SRM University, Kattankulathur-603203
Chennai, TamilNadu, India.
E-mail: neppolian.b@res.srmuniv.ac.in

Prof. Sami Rtimi
Professor
Swiss Federal Institute of Technology (EPFL),
Switzerland
Email: sami.rtimi@epfl.ch

Correlation preparation parameters/activity for microTiO_2 decorated with SilverNPs for NOx photodegradation under LED light

Giuseppina Cerrato[1], Federico Galli[3], Daria C. Boffito[2], Lorenza Operti[1], Claudia L. Bianchi[3*]

[1]Università degli Studi di Torino, Dipartimento di Chimica & NIS Interdept. Centre, via P. Giuria 7, 10125 Torino, Italy

[2]Polytechnique Montréal – Department of Chemical Engineering, C.P. 6079, Centre ville H3C 3A7 Montréal (QC) Canada

[3]Università degli Studi di Milano, Dipartimento di Chimica, via Golgi 19, 20133 Milano, Italy

* claudia.bianchi@unimi.it

Abstract

TiO_2 photocatalysts degrade pollutants in both the gas and liquid phase under UV radiation. To widen their application under solar and/or LED light, TiO_2 surface decoration with noble metals offers a mean to achieve such a goal. Ag species as a decorating agent improve TiO_2-based systems photoactivity and exhibit antibacterial properties under LED light and even in the dark. Ample literature is available on the synthesis of silver nanoparticles (Ag NPs) but few data are available on the interaction of such particles with micrometric samples. Indeed, micrometric samples pose less environmental and health concerns than the nano-sized powders widely adopted. The synthetic routes employed for Ag NPs decoration onto TiO_2 clearly influence the photocatalytic activity, in particular referring to both NPs shape and fine structure. Thus, we report the preparation of Ag NPs by an electrochemical method followed by the subsequent decoration onto a micrometric TiO_2 (Kronos 1077): different parameters, such as pH and the nature of physical nanoparticle dispersants were taken into account to evaluate their effect on the resulting Ag NPs features. We evaluated the photocatalytic activity towards the photodegradation of NOx under LED light, concluding that the best output was obtained by photocatalysts synthesised at basic pH.

1. Introduction

Capturing renewable sunlight by permanently abducting photons into complex systems capable of storing them and, at the same time, realizing them or transforming them into reactive species would arguably be the Holy Grail of energy utilization of the current century.

Researchers are looking for more efficient ways to store and re-use solar energy. Photocatalysis, still far from being efficient, offers scientists the chance of embracing this challenge [1]. In particular, TiO_2 is now seen as an unforsaken vector to attain the objective of an affordable and efficient photocatalyst.

TiO_2 undoubtedly possesses alluring characteristics such as long-term mechanical and thermal stability, even under irradiation [2], availability, feasible synthesis and low cost [3]. However, its low efficiency ejects widespread commercial applications. The reason of its inadequacy lies in its wide band-gap (Eg), which limits the irradiation that can be absorbed. Indeed, an $Eg \approx 3.2$ eV requires $\lambda_{irr} < 385$ nm, which disqualifies 95 % of the solar spectrum. In addition, the high recombination rate of the photogenerated species results in a low production rate of secondary photo-generated reactive compounds [4,5]. Diverse approaches such as coupling TiO_2 with other semiconductors [6,7], dye sensitizing [8,9], ion implantation [10], noble metal [4] decoration, doping with heteroatoms [11] now account for several literature data. Among the noble metals Ag NPs have been a target since they also possess antibacterial properties [12]. However, besides this, AgNPs exhibit the surface plasmon band typical of noble metal NPs, which originates from the Mie absorption in the visible spectrum. When incorporated onto TiO_2, its band-gap decreases, opening up the light absorption over a wider light spectrum region. The fundamental mechanism of visible light absorption by TiO_2 decorated with Ag identifies with the injection of metal plasmonic electrons into the wide band-gap semiconductor. However, the plasmonic absorption, which is an optical property at the surface/bulk interface, only manifest for NPs bigger than 2 nm. Below this size, quantum effects prevails [13]. The most recent approaches focus on interposing a layer of conductive material between TiO_2 and Ag to provide a conductive path for the electrons from the noble metal to the TiO_2 surface. For instance, Lang et al. intercalated graphene oxide (GO) nanosheets as bridges between Ag nanocubes and TiO_2 nanosheets to provide a conductive path for the electrons from the plasmonic Ag band to the

semiconductor [14]. Asapu et al. fabricated core-shell super stable Ag-TiO_2-PAH where polyallylaminehydrochloride (PAH) constitute a polycation layer [15], whereas Jbeli et al. Intercalated a chitosan film that formed an AgCl layer between TiO_2 and Ag species [16].

Controlling the dispersion and size of the noble metal over TiO_2 is fundamental to both maximize photocatalytic activity by tackling the mass transfer of active primary and secondary photogenerated species, as well limiting the input of catalyst precursors' and solvents in an approach towards sustainability. For instance, Stucchi et al. doped micrometric (110 nm) TiO_2 with Ag nanoparticles (NPs) in the weight range from 1 to 20 % by means of ultrasound [17]. Zeng et al. synthesized Ag nanowires with TiO_2 NPS around them that were stable for several days and degraded acetaldehyde in few minutes in gas phase under fluorescent light [18].

AgNPs agglomerated electrochemically to control their size is an innovative and interesting approach because it is possible to precisely control the size of Ag. Starowicz et al. polarized a sacrificial anode of Ag and obtained AgNPs of about 20 nm [19]. With the same technique, Rodriguez-Sanchez et al. obtained nanoparticles in the range 2-7 nm in acetonitrile and tetrabutylammonium bromide as electrolyte and stabilizer [19]. TiO_2 particle size is another fundamental issue to tackle the benefits of nanotechnology dominate our thinking nowadays. The concerns regarding nano-particles (< 100 nm) deal with inhalation and skin contact of particles that are so small to be potentially not "recognizable" by the human body barriers, thus reaching the organism cells. The number of papers on the subject "TiO_2 nanoparticles and toxicity", which raised from 57 (within 2008) to 985 in the last 10 years [Scopus.com source], is a proof of the increasing concern about the effects of nano-particles on living beings. Concurrently, major national and international agencies in Europe are promoting research on potential adverse effects of nanoparticles [20]. The effects of nano-sized TiO_2 on human health have not been fully demonstrated yet, but the first data on the adverse effect of nano-sized TiO_2 on animals just became available [21,22].

The authors recently confronted this issue by several papers published on increasing the photoactivity of micro-TiO_2 [23–25], whereby doping micro-sized TiO_2 the activity increased in the visible range.

Among all the pollutants, nitrogen oxides (NOx) are continuously monitored all over the world and guidelines on the alarm levels of these molecules in air were published by WHO [26] and

often recalled in the legislations of single countries worldwide. Photocatalysis with titanium dioxide as a semiconductor seems to be a promising technique to reduce the pollutant concentration due to its powerful oxidation properties. For this reason, the NOx degradation reaction was selected to probe the photocatalytic activity of our samples. Folli et al [27] report a correlation between the maximum NO removal (minimum concentration) with the maximum UV irradiance. Another recent review contribution by Schreck et al. [28] reports about NOx emissions, in particular from the transport sector, as they significantly impact the urban air quality. The band-gap of anatase phase TiO2 is 3.2 eV and the oxidation and reduction potentials of the valance and conduction bands are +2.95 V and −0.25 V, respectively. The reduction potential of NO to N2 is +3.36 V and the oxidation potential of NO to NO3− is −0.934 V indicating that both photooxidation and photoreduction of NO are feasible reactions over TiO_2 [29].

In this paper, we report the electrochemical synthesis of Ag NPs together with their subsequent deposit by incipient wetness on micrometric TiO_2. During the synthesis of the catalyst, the pH was varied in the 4-12 range, observing exceptional catalytic performance (90% NOx conversion in 1 h) under LED light for the sample obtained at pH = 14 and PVP/Ag+ molar ratio = 3.

2. Experimental

2.1 Silver nanoparticles preparation

Ag NPs were prepared from an $AgNO_3$, polyvinyl pyrrolidone (PVP) and KNO_3 solution. KNO_3 (≥ 99.0 %) and PVP (average molecular weight = 40 000) were purchased from Sigma Aldrich and were employed them with no further purification. 100 mL of a 30 g/L $AgNO_3$ solution were placed into a becker containing 1 g of KNO_3 and a weighted amount of PVP. KNO_3 solution was added as supporting electrolyte. PVP acted as physical nanoparticle dispersant [30] and we varied its concentration to gauge the effect of PVP on the synthesis. We varied the dispersant to understand its influence on the stabilization of Ag NPs. We selected polyvinyl alcohol (PVA) (average molecular weight = 9000-10000, 80% hydrolysed, Sigma Aldrich) [31] and polyacrylic acid (PAA, sodium salt, average molecular weight = 8000, Sigma Aldrich) [32]. The counter and working electrode were two platinum foils (40 mm x 20 mm), while the reference electrode was

a saturated calomel electrode (SCE). To protect SCE from AgCl precipitation, we used double bridge filled up with a saturated KNO_3 solution, which acted as second electrolyte.

AUTOLAB potentiostat coupled with Nova software determined the reduction potential for each test through cyclovoltammetry (CV). The cyclic staircase started from 0.4 V, reached a lower potential -0.2 V, increased until 1.0 V, and returned to 0.4 V. The reductive current obtained from CVs was almost constant from + 0.3V to - 0.2V, therefore it was decided to synthetize Ag nanoparticles at +0.2 V, to maximize silver production and to avoid, at the same time, to deposit metallic silver on the electrode. We observed that in this condition, after 10 min, silver only deposited on the working electrode. Therefore, we set the duration of each synthesis to 10 min.

We also modified the pH of the solution after the electrochemical synthesis with either HNO_3 or NH_4OH, to study the influence of pH on the Ag nanoparticles structure/morphology and verify its possible influence of the final photocatalytic performance.

2.2 Catalyst synthesis

During the electrochemical synthesis, the colour of the mixture gradually shifted from white to yellow and became cloudier, thus indicating the formation of nanoparticles. [3].

We then added NH_4OH to the silver nanoparticles (Ag NPs) solution to a pH of 12 to form NH_3. Ammonia stabilizes the dopant in the solution avoiding the formation of Ag_2O precipitate according to Tollens reaction (1-2):

$$2\ AgNO_3 + 2\ OH^- \rightarrow Ag_2O(s) + 2\ NO_3^- + H_2O \quad (1)$$

$$Ag_2O(s) + 4\ NH_3 + 2\ NO_3^- + H_2O \rightarrow 2\ [Ag(NH_3)_2]NO_3 + 2\ OH^- \quad (2)$$

We then suspended TiO_2 (Kronos 1077) in 6 mL of acetone (HPLC grade, Sigma Aldrich). We added the Ag NPs aqueous solution to the suspension to obtain an AgNPs mass loading of 8 % (value optimized in previous works). The solution was kept under stirring for 24 h, at a temperature of 40 °C. After, we raised the temperature to 80 °C for 2 h. At the end of the impregnation, we removed water by evaporation, and heated the mixture to 100 °C. A furnace calcined the powder at 400 °C for 2 h under static atmosphere.

Here we compare 7 catalysts (Table 1) prepared with different conditions. Sample 7 was prepared in the same condition of sample 6 but with 5 times the reagents amount and the volumes (500 mL of $AgNO_3$ solution, 5 g of KNO_3 and 40 cm^2 of working electrode surface) so to verify a possible modification of the final result after a simple scale-up.

Table 1: Synthesis of the Ag-TiO_2 samples.

Sample	Ag NPs loading (% by weight)	mol PVP / mol Ag^+	pH
1	0	-	-
2	8	3:1	12
3	8	50:1	12
4	8	3:1	4
5	8	1:1	4
6	8	1:1	12
7	8	1:1	12

2.3 Characterization

A JEOL 3010–UHR Instrument fitted with a LaB6 filament (acceleration potential 300 kV) and equipped with an Oxford INCA Energy TEM 200 energy dispersive X–ray (EDX) detector (TEM-HRTEM) imaged the samples. Samples were dry dispersed onto Cu grids coated with "lacey" carbon film.

A PANalytical Xpert Multipurpose X-ray Diffractometer measured samples crystallinity. It is equipped with a Cu anode (Kα radiation, λ = 1.54060 nm). The working potential was 45 kV while the working current was 40 mA. We analyzed our samples with a scan rate of 0.05° in a 2θ range of 20°-80°.

An M-Probe (SSI) XPS instrument was used to analyze the samples surfaces detecting in particular Ti_{2p}, O_{1s} and Au_{4f} regions. The instrument is equipped with a monochromatic $Al_{k\alpha}$ anode and is calibrated using C_{1s} at 284.6 eV.

Specific surface area measurements were carried out by conventional N_2 adsorption/desorption (BET) at 77 K by means of a Sorptometer (Costech Mod. 1042) apparatus.

A Thermo Scientific Evolution 600 spectrophotometer equipped with a diffuse reflectance accessory Praying-Mantis sampling kit measured the absorbance, (Harrick Scientific Products, USA). The reference material was a Spectralon1 disk.

2.4 NOx setup

We adopted a 20 L Pyrex glass batch reactor to degrade NOx. The complete description of the setup is reported elsewhere [33] and its scheme is available in the Supporting Information file (S4). We deposited a suspension of (0.050 ±0.001) mg of catalyst in isopropanol (technical grade, Sigma Aldrich) on a glass plate (200 mm x 20 mm). An ultrasonic bath suspended the powder in the alcohol before the deposition. After the evaporation of the solvent, we placed the plate with the catalyst on the top of it inside the reactor. The concentration of the model pollutant was 500 ppb of NOx (initial bottle concentration 0.625 % of NO_2 and 0.125 % of NO, diluted with air). A LED lamp (MW mean well, 350 mA rated current, 9 V to 48 V DC voltage range, 16:8W rated power) with an emission from 400 nm to 700 nm was the photon source set at a distance to have 1000 lux on the sample surface. We set the relative humidity of the reactor at 50 %. Time 0 corresponded to the switching on of the lamp. An Ecotech Serinus 40NOx directly connected to the reactor measured the concentration of both NO and NO_2 at 60, 180 and 360 min.

The calibration of the instrument was verified by sampling directly from the NOx cylinder to the instrument. The concentration of NOx matched the one declared by the gas supplier. The sampling was realized by opening a valve to let the instrument automatically withdraw a gas aliquot from the reactor. The lower detection limit of the instrument is 0.4 ppb and a precision of 0.5 % [34]. Therefore, we calculated the error on the NOx conversion using the formula for the error propagation.

3. Results and discussion

3.1 Selection of the capping agent

The electrochemical synthesis of AgNPs failed with PAA and PVA for different reasons. The carboxylic domains of PAA exchanged sodium ion with silver ion in the solution and formed an insoluble complex that precipitated [35]. PVA did bring to the formation of an AgNPs solution, but that was in turn unstable. For all the concentrations tested, the NPs coagulated and aggregated within 3-4 hours. Literature reports stability for the Ag-PVA complex with increasing dispersant molecular weight and when other rheological additive are present [36]. We filed the synthesis with different concentration of PVA (from 10 to 30 g L^{-1}). We therefore selected PVP for all the synthesis.

3.2 Sample morphology and nanoparticle size distribution

All the samples object of the present research exhibit almost the same value (~ 12 ± 2 m^2 g^{-1}) of BET specific surface area, i.e. the value related to the bare TiO_2 (micrometric sample 1) despite the presence of Ag NPS.

TEM confirmed that the average dimensions for sample 1 (i.e., bare Kronos 1077) are around 110 nm. Its particles are well ordered, in most cases they are thin and not too much closed packed together. A detailed inspection at higher magnification (see Supporting Information Fig S1) indicates that all the particles are highly crystalline: the calculated distances (0.35_2 nm) among the fringes evidence that the most frequently exposed crystal planes belong to the (101) family of anatase [ICDD 21-1272]. This feature is also confirmed by the analysis of the electron diffraction.

The general morphology of the supporting material remains unchanged for Sample 2, despite the procedure followed to add silver species. Sample 2 exhibits the same external habit of the titania crystals reported for sample 1 and the same fringe patterns ascribable to anatase (see Figure 2b).

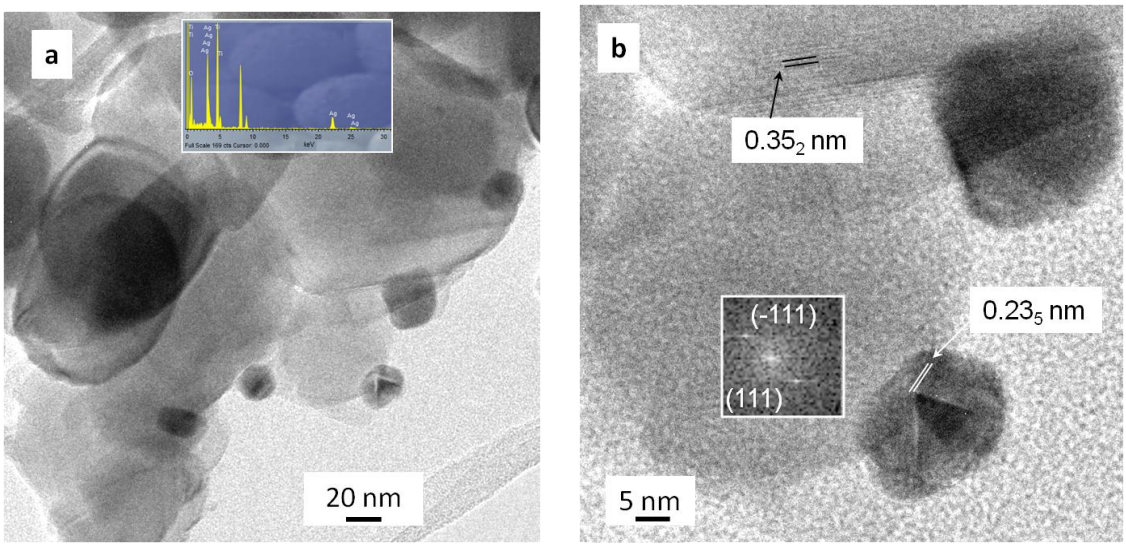

Figure 2. C-TEM (section a) and HR-TEM (section b) images referred to sample 2.

The extra particles present in Figure 2a, characterized by a much lower size and higher contrast as well, are made up of Ag. This is confirmed by different experimental evidences: (i) the EDX analysis, reported in the inset to Figure 2a, indicates the presence of metallic Ag, besides Ti and O; (ii) the inspection of the fringe patterns exhibited by the smaller particles (Figure 2b) puts into evidence that the calculated 0.23 nm distances are ascribable to metallic silver [ICDD 004-0783]. Sample 3 resembles sample 2 (Figure 3). Both samples have been synthesized in similar pH (basic) conditions but with different PVP.

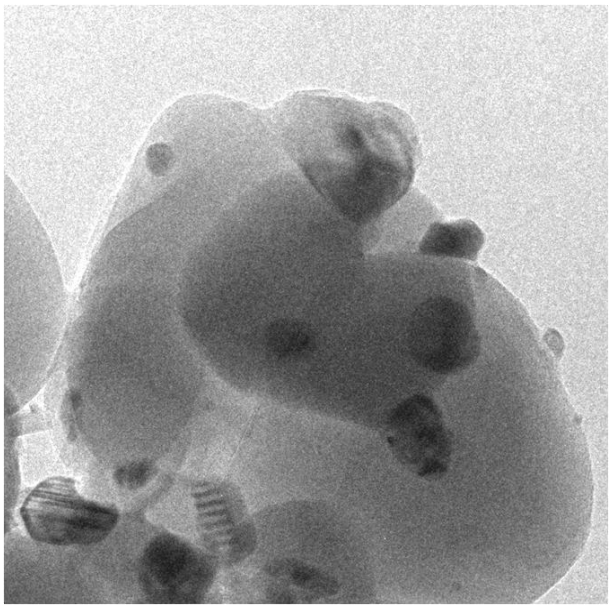

Figure 3. C-TEM image referred to sample 3

Samples 4 and 5 were synthetized in acidic conditions. Their morphology confirms to be unaltered for the titania support, but deeply different for what concerns the Ag NPs appearance (see Figure 4 and 5, respectively). In fact, their size is much smaller, being far beyond a half than in the case of the samples obtained at basic pH.

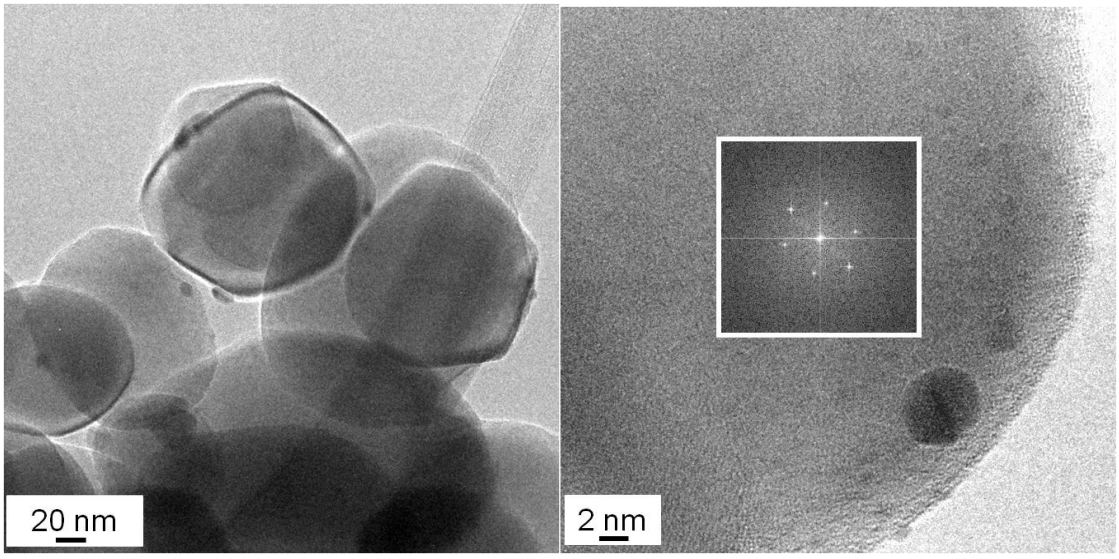

Figure 4. C-TEM (section a) and HR-TEM (section b) images referred to sample 4.

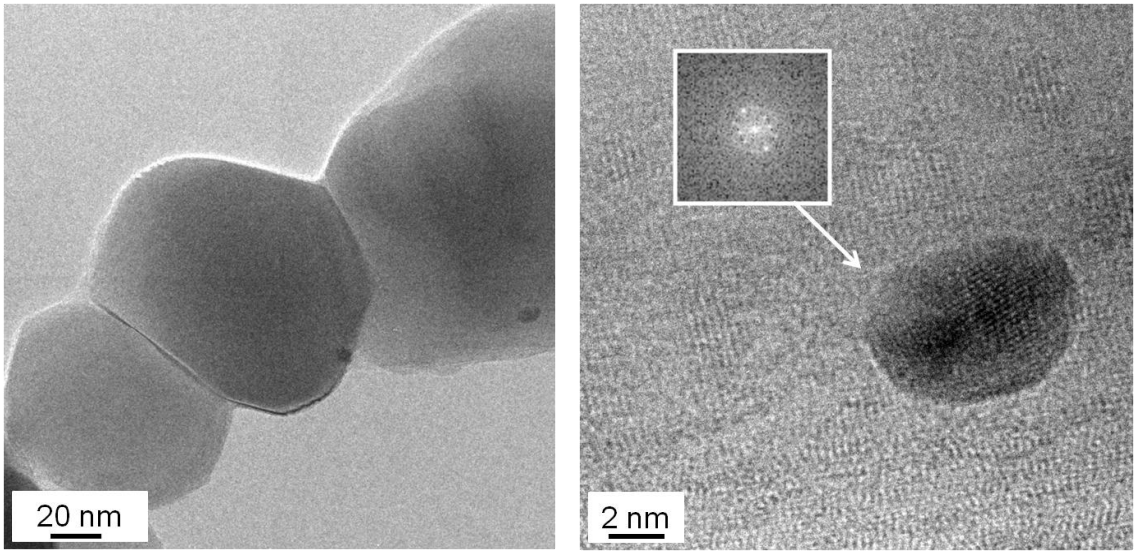

Figure 5. C-TEM (section a) and HR-TEM (section b) images referred to sample 5.

In the case of sample 6 the situation is intermediate between the two above described: see Figure 6. Sample 7 shows the same morphology of sample 6 confirming that the scale-up process does not alter the AgNPs features.

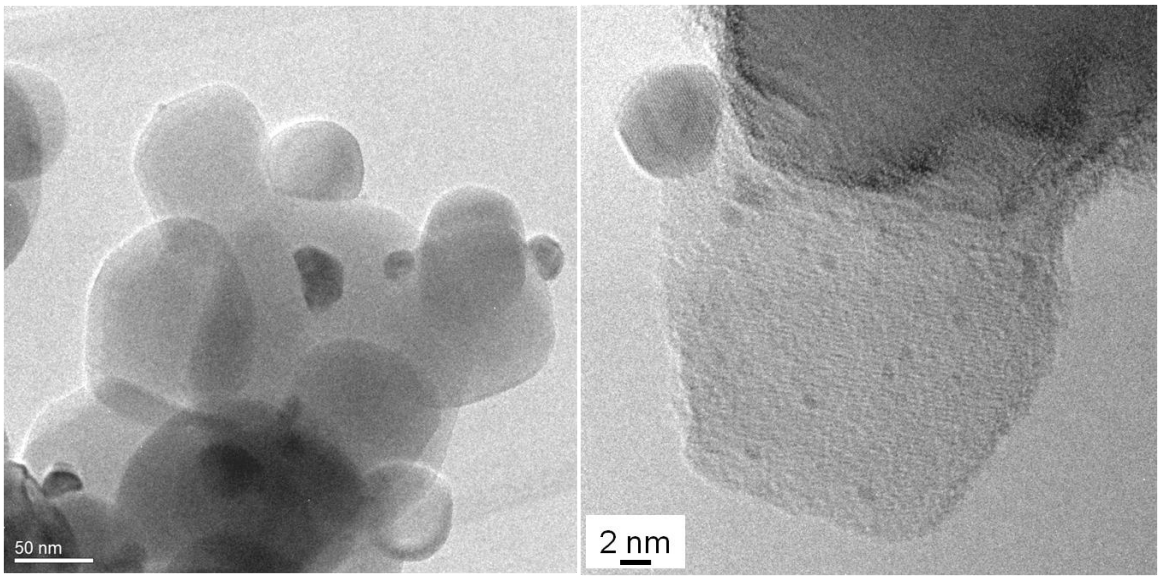

Figure 6. C-TEM (section a) and HR-TEM (section b) images referred to sample 6.

For samples 2, 3 and 6 (and 7) there is a broader spread of Ag NPs dimensions, ranging in the 5-25 nm (with dominating dimensions in the 15-20 nm range, Supporting Information Figure S2) with respect to samples 4 and 5, for which the distribution is much narrower and whose mean size is located in the 1-5 nm range.

The amount of silver in the various preparations (Table 1) was constant ($8\%_{wt}$), whereas the parameters that have been changed are either the amount of the PVP dispersing agent or the pH of the solutions before the electrochemical synthesis.

In the condition of constant pH (no matter acidic or basic), the effect of a different amount of PVP is almost negligible, as the relevant AgNPs distribution are similar for the two pH values. Our results hold also considering diverse AgNPs preparation methods. Malina et al. [37] reduced

$AgNO_3$ with $NaBH_4$ varying the concentration of PVP. They did not see a significant change in AgNPs size below a concentration of 10 % of PVP. Moreover, changing PVP concentration leads to similar NPs distribution during the laser ablation preparation method [38].

On the other hand, the different pH values have a great influence in the Ag NPs distributions. In fact, changing pH from 11.5 to 12.5 leads to bigger nanoparticles when the reducing agent is a sugar [39]. Therefore, pH possesses a leading role in determining the ultimate size(s) of the AgNPs, during the direct electrochemical reduction of $AgNO_3$.

The crystallographic phase composition of the various samples has been assessed also based on the X-Ray diffraction investigation: Figure 7 summarizes the relevant results for the 2 to 5 powders.

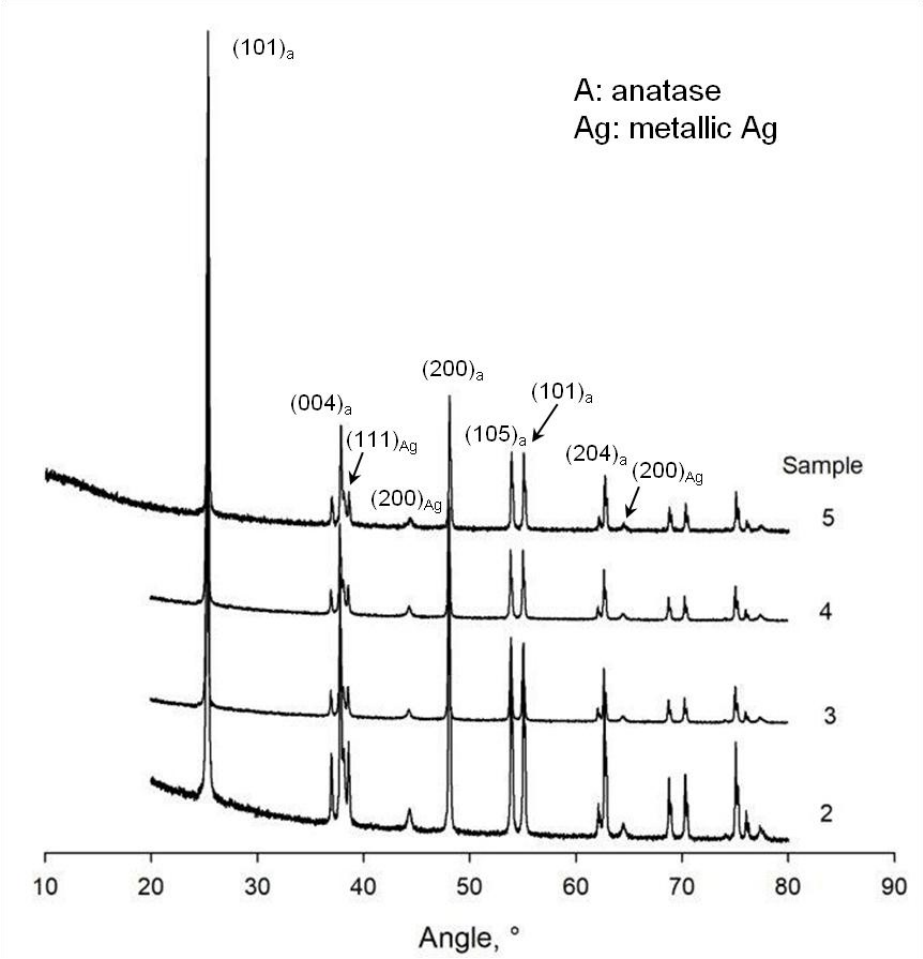

Figure 7: XRD of samples 2-5.

It is well evident that the main features are ascribable to the anatase TiO_2 polymorph, as expected also on the basis of the morphological characterization carried out by means of HR-

TEM investigation. In all the diffractograms, the main peak at 2θ ~ 25° can be ascribed to the most intense (101) peak due to anatase [ICDD card n. 21-1272], as well as many other reflexes: a few differences in intensity for the minor peaks is observable, but this is the only peculiarity that can be evidenced in particular for sample 4 and 5, synthesized in acidic conditions. Besides these peaks, a clear indication of the presence of metallic Ag comes from the three reflexes located at 2θ ~ 38°, 44 ° and 65°, respectively ascribable to (111), (200) and (200) crystal planes [on the basis of metallic Ag ICDD card n. 4-0783]. No extra peaks are observable that can indicate the presence of oxidated Ag species: this fact may be due to the very low amount of these species (if present most likely due to passivation effects), lying then under the detection power of the XRD technique. For this reason, we resorted the XPS analysis in order to shed some light onto this feature.

High-resolution XPS for O 1s region (sample 6) is the sum of three contributions: a main peak centred at 530 eV, representing the lattice oxygen of TiO_2, a less intense shoulder peak with binding energy at 531 eV, corresponding to the lattice oxygen of Ag_xO, and a third shoulder peak at 532 eV, related to OH species [40] (Fig. 8 right).

Ti 2p spectrum (Supporting Information, Figure S3) only highlights the presence of a single doublet typical of Ti^{4+} in TiO_2.

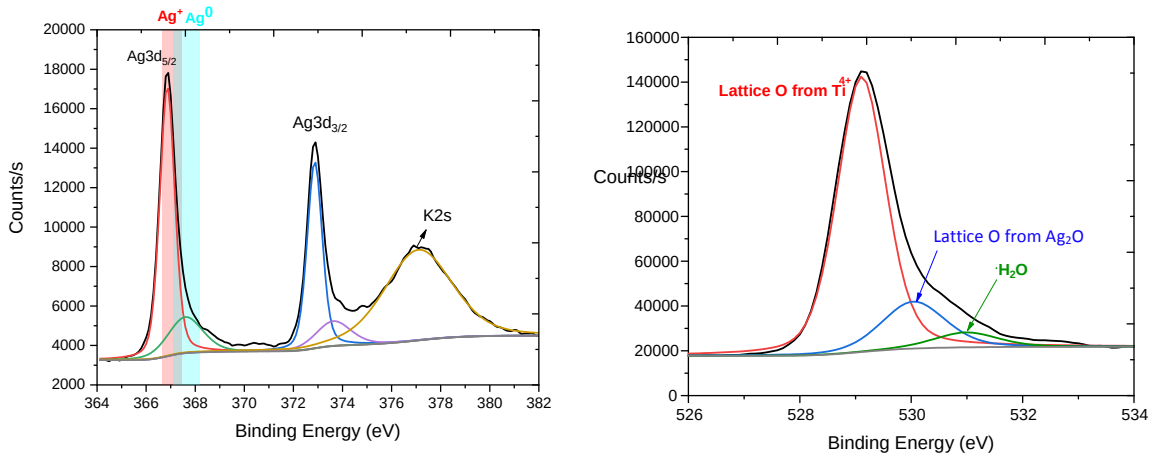

Figure 8: XPS High-resolution spectrum of O1s (right) and Ag3d (left) for sample 6

The ratio between the areas of the peaks located at 529 and 532 eV, respectively, gives useful information about the hydroxyl species (OH) located at the surface of the photocatalyst. In particular, if we compare the OH/O_{tot} ratio calculated for samples 6 and 1 (bare TiO_2), we obtain 0.06 and 0.32 [36], respectively: on the basis of this evidence, we can preliminary conclude sample 6 activity is related to the creation of oxyradicals in situ, favoured because of controlled humidity (50 %) (see the NOx degradation section).

The Ag3d XPS spectrum of sample 6 (Figure 8 left) fits into two separated peaks, one referring to Ag^0 and the other one to its higher valence state Ag^+/Ag_xO [35]. The presence of higher valence state Ag confirms the deduction made discussing the O1s XPS spectrum, due to the presence of a fitted peak at ~531 eV. Due to the calcination in air during the final preparation step, a mix of metal and oxidized Ag nanoparticles are present on the surface of the TiO_2 micro-particles. This morphological feature has not been evidenced by the HR-TEM inspection, as the fraction of oxidized AgNPs is most likely so low that lies under the detection power of this experimental technique.

A modification of the UV-Vis spectra is also evident (supporting information, Figure S5) with an increase of the adsorption at wavelengths in the visible range of 400 nm and 700 nm for all samples but mainly for sample 6.

3.3 NOx degradation

Bare 1077 micro TiO_2 (sample 1) is ineffective towards NOx degradation under visible light. Our result is comparable to the literature and confirms that this material is only active under UV light [33].

Sample 2 exhibits exceptional activity. It converts 90 % of NOx after 1 h of irradiation. Sample 3, 5 and 6 have similar kinetics, while sample 4 is the least active among the series (Figure 9 a). Sample 7 shows the same result of sample 6 even if it was prepared with 5 times the volumes of reagents. Therefore, the properties of this catalyst is unaffected by the volume of the synthesis.

All the catalysts tend to deactivate after 6 h due to the reaction mechanism that brings to the formation of nitrate species (NO_3^-), which we already detected in previous works employing photocatalytic tiles [33,41].

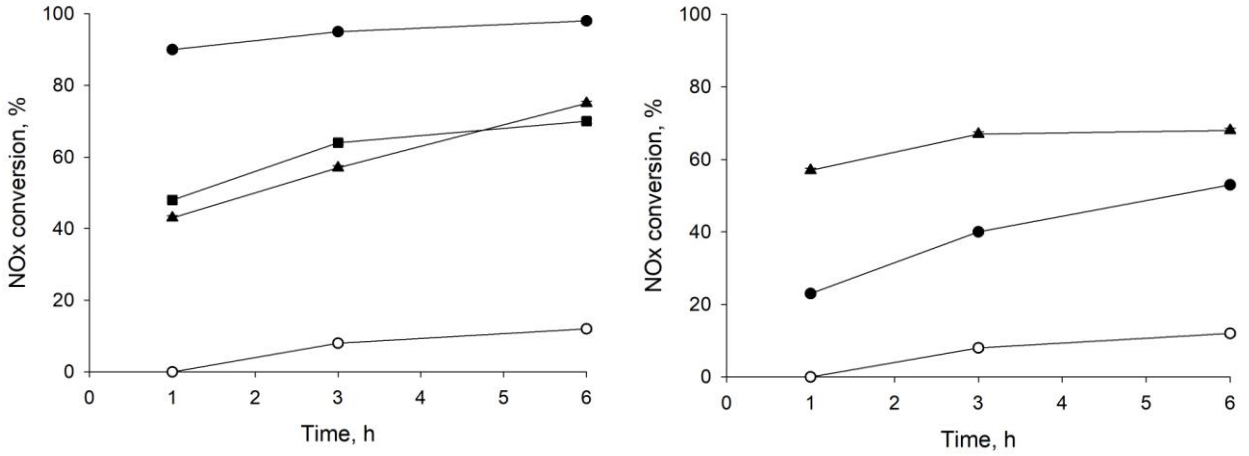

Figure 9 : NOx conversion versus time for catalysts prepared at basic (left side) and acid (right side) pH. Empty symbols correspond to Kronos 1077 while triangles, points and squares represent a PVP/Ag molar ratio of 1, 3 and 50, respectively.

Ag NPs, as well as gold NPs, degrade VOC through different mechanisms depending on the light source and their morphology [42]. Here, we adopted LED light, whose energy is insufficient to directly promote electrons to the valance band of TiO_2. Therefore, localized surface plasmon resonance (LSPR) absorption in Ag NPs is the main effect that makes our samples active. However, when nanoparticles cluster, the absorption is broader and covers a wavelength range of 350 – 500, a range that falls in the emission of the LED lamp employed in our study, which also contribute to their activity, even if to a lower extent.

The optimal PVP/Ag+ molar ratio at pH = 4 was 1, while at pH = 12 it becomes 3 (Figure 10). We hypothesize that this is connected to the particle dimensions. At acid pH, smaller particles form (1-5 nm), therefore less PVP is needed to stabilize them, even though their number is higher, and as a matter of fact, an AgNP size smaller than 5 nm leads to lower NOx conversions.

Sarina et al. correlated the conversion of a photocatalytic reaction (ethylene oxidation) to the plasmon intensity [42]. In another work, Amendola et al. calculated the LSPR of different AgNPs, varying their shapes and assemblies [43]. A single spherical AgNP (radius = 10 nm) absorbs light whose wavelength is between 350 and 450 nm. The same authors also demonstrated that AgNPs smaller than 5 nm, like the ones we obtained in the synthesis with pH

= 4, broaden the absorption band, which correlates with their lower performances compared to catalyst prepared at basic pH.

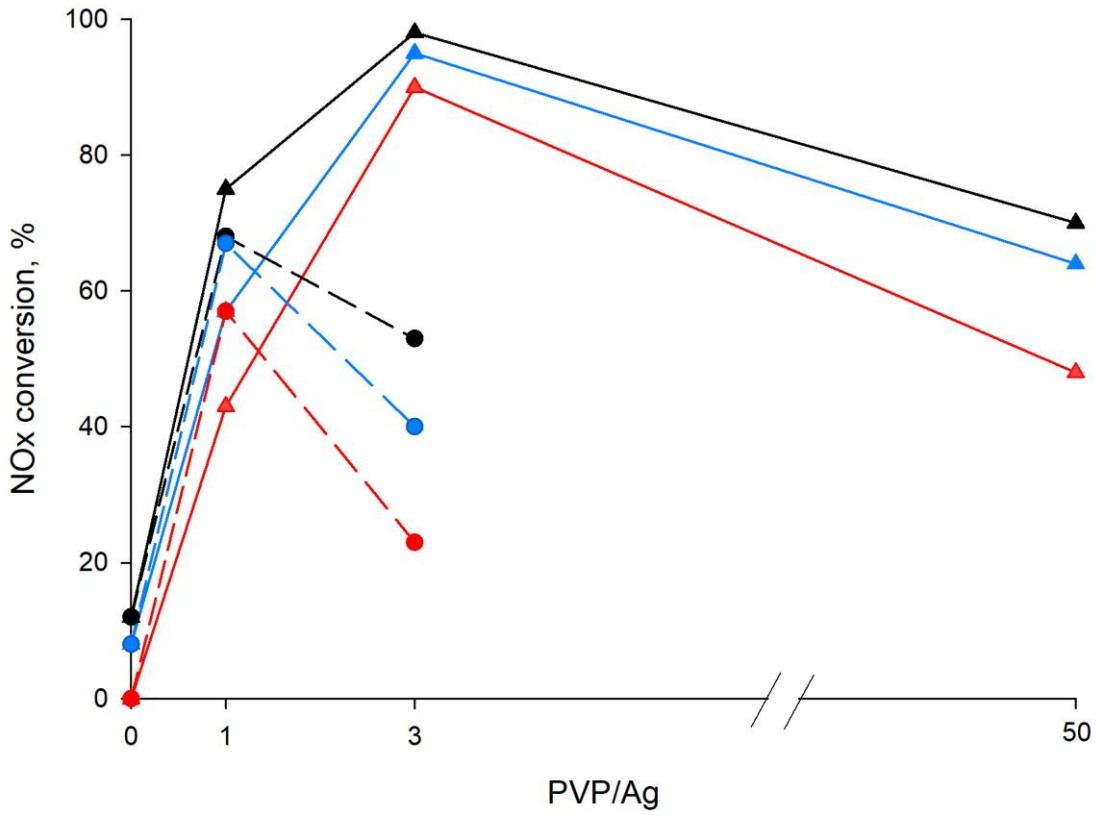

Figure 10: PVP/Ag molar ratio versus NOx conversion for acid pH (dotted lines and points) and basic pH (full line and triangles). Red, blue and black lines represent conversion at time 1 h, 3 h, and 6 h, respectively.

4. Conclusion

In the present contribution we synthetized AgNPs reducing silver nitrate in solution by an electrochemical method. The pH of the solution tailors the dimension of the nanoparticles. At pH = 4 we obtained a NPs distribution 1-5 nm, whereas at pH = 12 this figure becomes 5-25 nm. pH

and polyvinyl pyrrolidone has no influence on the crystallinity of samples and the calcination procedure we propose (400 °C for 2 h in air) yield stable nanoparticles.

As for the titania photocatalyst support, we decided to employ a micrometric commercial system (1077 by Kronos) rather than a nanometric powder, in order to avoid all the possible drawbacks typical of the interaction of NPs with human tissues by either inhalation or skin contact. The photocatalysts we obtained retain all the positive properties due to the micrometric support, such as SSA, crystallographic phase composition, being thus positively influenced in their photocatalytic performances by the promotion by AgNPs, even though a different photodegradation behaviour, as a function of the different AgNPs preparation route, has been put into evidence.

In particular, photocatalytic degradation of NOx under LED light evidenced that the samples prepared at basic conditions exhibit better performances rather than those prepared at acid conditions: AgNPs with diameters of 1-5 nm are less active under LED light because of the broadening of the surface plasmon band. Moreover, the synthesis was scaled up to 500 mL volume, without affecting the final catalysts performances.

Acknowledgements

The Authors acknowledge Projet de cooperation Quebec Italie 2017-2019 (project number: QU17MO09) for granting the mobility of researchers between Canada and Italy. This research was undertaken, in part, thanks to funding from the Canada Research Chairs program.

References

[1] G. Mamba, J. Kiwi, C. Pulgarin, R. Sanjines, S. Giannakis, S. Rtimi, Evidence for the degradation of an emerging pollutant by a mechanism involving iso-energetic charge transfer under visible light, Appl. Catal. B Environ. 233 (2018) 175–183. doi:10.1016/j.apcatb.2018.03.109.

[2] C. Pirola, D.C. Boffito, S. Vitali, C.L. Bianchi, Photocatalytic coatings for building industry: study of 1 year of activity in the NO x degradation, J. Coatings Technol. Res. 9 (2012) 453–458. doi:10.1007/s11998-011-9381-7.

[3] M. Hosseini-Sarvari, F. Jafari, A. Mohajeri, N. Hassani, Cu 2 O/TiO 2 nanoparticles as visible light photocatalysts concerning C(sp 2)–P bond formation, Catal. Sci. Technol. 8 (2018) 4044–4051. doi:10.1039/C8CY00822A.

[4] Z. Wei, M. Janczarek, M. Endo, K. Wang, A. Balčytis, A. Nitta, M.G. Méndez-Medrano, C. Colbeau-Justin, S. Juodkazis, B. Ohtani, E. Kowalska, Noble metal-modified faceted anatase titania photocatalysts: Octahedron versus decahedron, Appl. Catal. B Environ. 237 (2018) 574–587. doi:10.1016/j.apcatb.2018.06.027.

[5] Z. Song, B. Hong, X. Zhu, F. Zhang, S. Li, J. Ding, X. Jiang, J. Bao, C. Gao, S. Sun, CdS/Au/Ti/Pb(Mg1/3Nb2/3)0.7Ti0.3O3 photocatalysts and biphotoelectrodes with ferroelectric polarization in single domain for efficient water splitting, Appl. Catal. B Environ. 238 (2018) 248–254. doi:https://doi.org/10.1016/j.apcatb.2018.07.033.

[6] N. Saadatkhah, M.G. Rigamonti, D.C. Boffito, H. Li, G.S. Patience, Spray dried SiO 2 WO 3 /TiO 2 and SiO 2 vanadium pyrophosphate core-shell catalysts, Powder Technol. 316 (2017) 434–440. doi:10.1016/j.powtec.2016.10.056.

[7] H. Khan, M.G. Rigamonti, G.S. Patience, D.C. Boffito, Spray dried TiO 2 /WO 3 heterostructure for photocatalytic applications with residual activity in the dark, Appl. Catal. B Environ. 226 (2018) 311–323. doi:10.1016/j.apcatb.2017.12.049.

[8] Z. Wang, X. Lang, Visible light photocatalysis of dye-sensitized TiO2: The selective aerobic oxidation of amines to imines, Appl. Catal. B Environ. 224 (2018) 404–409. doi:10.1016/j.apcatb.2017.10.002.

[9] X. Li, J.-L. Shi, H. Hao, X. Lang, Visible light-induced selective oxidation of alcohols with air by dye-sensitized TiO 2 photocatalysis, Appl. Catal. B Environ. 232 (2018) 260–267. doi:10.1016/j.apcatb.2018.03.043.

[10] A. Utsunomiya, A. Okemoto, Y. Nishino, K. Kitagawa, H. Kobayashi, K. Taniya, Y. Ichihashi, S. Nishiyama, Mechanistic study of reaction mechanism on ammonia photodecomposition over Ni/TiO 2 photocatalysts, Appl. Catal. B Environ. 206 (2017) 378–383. doi:10.1016/j.apcatb.2017.01.045.

[11] I. Milošević, S. Rtimi, A. Jayaprakash, B. van Driel, B. Greenwood, A. Aimable, M.

Senna, P. Bowen, Synthesis and characterization of fluorinated anatase nanoparticles and subsequent N-doping for efficient visible light activated photocatalysis, Colloids Surfaces B Biointerfaces. 171 (2018) 445–450. doi:10.1016/j.colsurfb.2018.07.035.

[12] S. Rtimi, D.D. Dionysiou, S.C. Pillai, J. Kiwi, Advances in catalytic/photocatalytic bacterial inactivation by nano Ag and Cu coated surfaces and medical devices, Appl. Catal. B Environ. 240 (2019) 291–318. doi:10.1016/j.apcatb.2018.07.025.

[13] A. Moores, F. Goettmann, The plasmon band in noble metal nanoparticles: an introduction to theory and applications, New J. Chem. 30 (2006) 1121. doi:10.1039/b604038c.

[14] Q. Lang, Y. Chen, T. Huang, L. Yang, S. Zhong, L. Wu, J. Chen, S. Bai, Graphene "bridge" in transferring hot electrons from plasmonic Ag nanocubes to TiO2 nanosheets for enhanced visible light photocatalytic hydrogen evolution, Appl. Catal. B Environ. 220 (2018) 182–190. doi:10.1016/j.apcatb.2017.08.045.

[15] R. Asapu, N. Claes, S. Bals, S. Denys, C. Detavernier, S. Lenaerts, S.W. Verbruggen, Silver-polymer core-shell nanoparticles for ultrastable plasmon-enhanced photocatalysis, Appl. Catal. B Environ. 200 (2017) 31–38. doi:10.1016/j.apcatb.2016.06.062.

[16] A. Jbeli, Z. Hamden, S. Bouattour, A.M. Ferraria, D.S. Conceição, L.F.V. Ferreira, M.M. Chehimi, A.M.B. do Rego, M. Rei Vilar, S. Boufi, Chitosan-Ag-TiO2 films: An effective photocatalyst under visible light, Carbohydr. Polym. 199 (2018) 31–40. doi:10.1016/j.carbpol.2018.06.122.

[17] M. Stucchi, C.L. Bianchi, C. Argirusis, V. Pifferi, B. Neppolian, G. Cerrato, D.C. Boffito, Ultrasound assisted synthesis of Ag-decorated TiO2 active in visible light, Ultrason. Sonochem. 40 (2018) 282–288. doi:10.1016/j.ultsonch.2017.07.016.

[18] Q. Zeng, X. Xie, X. Wang, Y. Wang, G. Lu, D.Y.H. Pui, J. Sun, Enhanced photocatalytic performance of Ag@TiO2 for the gaseous acetaldehyde photodegradation under fluorescent lamp, Chem. Eng. J. 341 (2018) 83–92. doi:10.1016/j.cej.2018.02.015.

[19] M. Starowicz, B. Stypuła, J. Banaś, Electrochemical synthesis of silver nanoparticles, Electrochem. Commun. 8 (2006) 227–230. doi:10.1016/j.elecom.2005.11.018.

[20] K. Ozawa, M. Emori, S. Yamamoto, R. Yukawa, S. Yamamoto, R. Hobara, K. Fujikawa,

H. Sakama, I. Matsuda, Electron–Hole Recombination Time at TiO 2 Single-Crystal Surfaces: Influence of Surface Band Bending, J. Phys. Chem. Lett. 5 (2014) 1953–1957. doi:10.1021/jz500770c.

[21] F. Hong, L. Wang, Nanosized titanium dioxide-induced premature ovarian failure is associated with abnormalities in serum parameters in female mice, Int. J. Nanomedicine. Volume 13 (2018) 2543–2549. doi:10.2147/IJN.S151215.

[22] P. Sá-Pereira, M.S. Diniz, L. Moita, T. Pinheiro, E. Mendonça, S.M. Paixão, A. Picado, Protein profiling as early detection biomarkers for TiO2 nanoparticle toxicity in Daphnia magna, Ecotoxicology. 27 (2018) 430–439. doi:10.1007/s10646-018-1907-7.

[23] M. Stucchi, D. Boffito, E. Pargoletti, G. Cerrato, C. Bianchi, G. Cappelletti, Nano-MnO2 Decoration of TiO2 Microparticles to Promote Gaseous Ethanol Visible Photoremoval, Nanomaterials. 8 (2018) 686. doi:10.3390/nano8090686.

[24] G. Cerrato, C.L. Bianchi, F. Galli, C. Pirola, S. Morandi, V. Capucci, Micro-TiO2 coated glass surfaces safely abate drugs in surface water, J. Hazard. Mater. 363 (2019) 328–334. doi:10.1016/j.jhazmat.2018.09.057.

[25] M. Stucchi, C.L. Bianchi, C. Pirola, S. Vitali, G. Cerrato, S. Morandi, C. Argirusis, G. Sourkouni, P.M. Sakkas, V. Capucci, Surface decoration of commercial micro-sized TiO2 by means of high energy ultrasound: A way to enhance its photocatalytic activity under visible light, Appl. Catal. B Environ. 178 (2015) 124–132. doi:10.1016/j.apcatb.2014.10.004.

[26] WHO, Ambient (outdoor) air quality and health, (2018). https://www.who.int/news-room/fact-sheets/detail/ambient-(outdoor)-air-quality-and-health (accessed February 1, 2019).

[27] A. Folli, J.Z. Bloh, M. Strøm, T. Pilegaard Madsen, T. Henriksen, D.E. Macphee, Efficiency of Solar-Light-Driven TiO 2 Photocatalysis at Different Latitudes and Seasons. Where and When Does TiO 2 Really Work?, J. Phys. Chem. Lett. 5 (2014) 830–832. doi:10.1021/jz402704n.

[28] M. Schreck, M. Niederberger, Photocatalytic Gas Phase Reactions, Chem. Mater. (2019)

acs.chemmater.8b04444. doi:10.1021/acs.chemmater.8b04444.

[29] N. Bowering, G.S. Walker, P.G. Harrison, Photocatalytic decomposition and reduction reactions of nitric oxide over Degussa P25, Appl. Catal. B Environ. 62 (2006) 208–216. doi:10.1016/j.apcatb.2005.07.014.

[30] B. Yin, H. Ma, S. Wang, S. Chen, Electrochemical Synthesis of Silver Nanoparticles under Protection of Poly(N -vinylpyrrolidone), J. Phys. Chem. B. 107 (2003) 8898–8904. doi:10.1021/jp0349031.

[31] R. Surudzic, Z. Jovanovic, N. Bibic, B. Nikolic, V. Miskovic-Stankovic, Electrochemical synthesis of silver nanoparticles in poly(vinyl alcohol) solution, J. Serbian Chem. Soc. 78 (2013) 2087–2098. doi:10.2298/JSC131017124S.

[32] S. Magdassi, M. Grouchko, O. Berezin, A. Kamyshny, Triggering the Sintering of Silver Nanoparticles at Room Temperature, ACS Nano. 4 (2010) 1943–1948. doi:10.1021/nn901868t.

[33] C.L. Bianchi, C. Pirola, F. Galli, G. Cerrato, S. Morandi, V. Capucci, Pigmentary TiO2: A challenge for its use as photocatalyst in NOx air purification, Chem. Eng. J. 261 (2015) 76–82. doi:10.1016/j.cej.2014.03.078.

[34] Ecotech, Serinus 40 brochure, (2018) 2. https://www.ecotech.com/wp-content/uploads/2015/03/ECOTECH-Serinus-40-NOx-Gas-Analyser-spec-sheet-20181202.pdf (accessed January 21, 2019).

[35] J.A. Dean, Lange's Handbook Of Chemistry, 15th ed., 1999.

[36] K.A. Juby, C. Dwivedi, M. Kumar, S. Kota, H.S. Misra, P.N. Bajaj, Silver nanoparticle-loaded PVA/gum acacia hydrogel: Synthesis, characterization and antibacterial study, Carbohydr. Polym. 89 (2012) 906–913. doi:10.1016/j.carbpol.2012.04.033.

[37] D. Malina, A. Sobczak-Kupiec, Z. Wzorek, Z. Kowalski, Silver nanoparticles synthesis with different concentrations of Polyvinylpyrrolidone, Dig. J. Nanomater. Biostructures. 7 (2012) 1527–1534.

[38] T. Tsuji, D.-H. Thang, Y. Okazaki, M. Nakanishi, Y. Tsuboi, M. Tsuji, Preparation of

silver nanoparticles by laser ablation in polyvinylpyrrolidone solutions, Appl. Surf. Sci. 254 (2008) 5224–5230. doi:10.1016/j.apsusc.2008.02.048.

[39] A. Panáček, L. Kvítek, R. Prucek, M. Kolář, R. Večeřová, N. Pizúrová, V.K. Sharma, T. Nevěčná, R. Zbořil, Silver Colloid Nanoparticles: Synthesis, Characterization, and Their Antibacterial Activity, J. Phys. Chem. B. 110 (2006) 16248–16253. doi:10.1021/jp063826h.

[40] H. Ren, P. Koshy, F. Cao, C.C. Sorrell, Multivalence Charge Transfer in Doped and Codoped Photocatalytic TiO 2, Inorg. Chem. 55 (2016) 8071–8081. doi:10.1021/acs.inorgchem.6b01200.

[41] C.L. Bianchi, C. Pirola, F. Galli, S. Vitali, A. Minguzzi, M. Stucchi, F. Manenti, V. Capucci, NO x degradation in a continuous large-scale reactor using full-size industrial photocatalytic tiles, Catal. Sci. Technol. 6 (2016) 2261–2267. doi:10.1039/C5CY01627D.

[42] S. Sarina, E.R. Waclawik, H. Zhu, Photocatalysis on supported gold and silver nanoparticles under ultraviolet and visible light irradiation, Green Chem. 15 (2013) 1814. doi:10.1039/c3gc40450a.

[43] V. Amendola, O.M. Bakr, F. Stellacci, A Study of the Surface Plasmon Resonance of Silver Nanoparticles by the Discrete Dipole Approximation Method: Effect of Shape, Size, Structure, and Assembly, Plasmonics. 5 (2010) 85–97. doi:10.1007/s11468-009-9120-4.

*Graphical Abstract

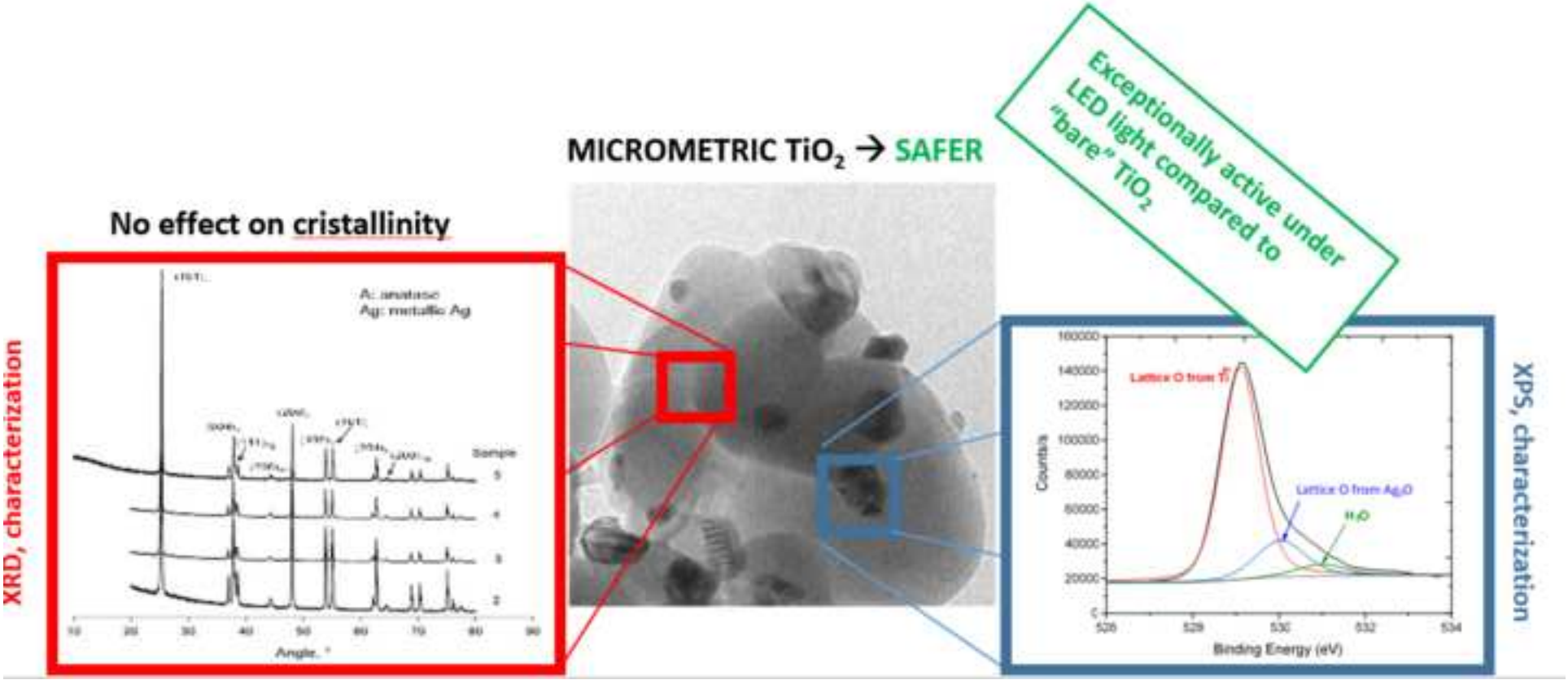

Correlation preparation parameters/activity for microTiO_2 decorated with SilverNPs for NOx photodegradation under LED light

Giuseppina Cerrato, Federico Galli, Daria C. Boffito, Lorenza Operti, Claudia L. Bianchi

Research Highlights

- Decoration of micro-sized TiO_2 with AgNPs using wet impregnation method.
- Preparation of AgNPs solution via electrochemical synthesis.
- The effect of pH on the NPs synthesis was evaluated.
- Excellent activity in the NOx photodegradation under LED light.

Supplementary Material

Click here to download Supplementary Material: Supp Info.docx

Correlation preparation parameters/activity for microTiO_2 decorated with SilverNPs for NOx photodegradation under LED light

Giuseppina Cerrato[1], Federico Galli[3], Daria C. Boffito[2], Lorenza Operti[1], Claudia L. Bianchi[3*]

[1]Università degli Studi di Torino, Dipartimento di Chimica & NIS Interdept. Centre, via P. Giuria 7, 10125 Torino, Italy

[2]Polytechnique Montréal – Department of Chemical Engineering, C.P. 6079, Centre ville H3C 3A7 Montréal (QC) Canada

[3]Università degli Studi di Milano, Dipartimento di Chimica, via Golgi 19, 20133 Milano, Italy

* claudia.bianchi@unimi.it

Abstract

TiO_2 photocatalysts degrade pollutants in both the gas and liquid phase under UV radiation. To widen their application under solar and/or LED light, TiO_2 surface decoration with noble metals offers a mean to achieve such a goal. Ag species as a decorating agent improve TiO_2-based systems photoactivity and exhibit antibacterial properties under LED light and even in the dark. Ample literature is available on the synthesis of silver nanoparticles (Ag NPs) but few data are available on the interaction of such particles with micrometric samples. Indeed, micrometric samples pose less environmental and health concerns than the nano-sized powders widely adopted. The synthetic routes employed for Ag NPs decoration onto TiO_2 clearly influence the photocatalytic activity, in particular referring to both NPs shape and fine structure. Thus, we report the preparation of Ag NPs by an electrochemical method followed by the subsequent decoration onto a micrometric TiO_2 (Kronos 1077): different parameters, such as pH and the nature of physical nanoparticle dispersants were taken into account to evaluate their effect on the resulting Ag NPs features. We evaluated the phocatalytic activity towards the photodegradation of NOx under LED light, concluding that the best output was obtained by photocatalysts synthesised at basic pH.

1. Introduction

Capturing renewable sunlight by permanently abducting photons into complex systems capable of storing them and, at the same time, realizing them or transforming them into reactive species would arguably be the Holy Grail of energy utilization of the current century.

Researchers are looking for more efficient ways to store and re-use solar energy. Photocatalysis, still far from being efficient, offers scientists the chance of embracing this challenge [1]. In particular, TiO_2 is now seen as an unforsaken vector to attain the objective of an affordable and efficient photocatalyst.

TiO_2 undoubtedly possesses alluring characteristics such as long-term mechanical and thermal stability, even under irradiation [2], availability, feasible synthesis and low cost [3]. However, its low efficiency ejects widespread commercial applications. The reason of its inadequacy lies in its wide band-gap (Eg), which limits the irradiation that can be absorbed. Indeed, an $Eg \approx 3.2$ eV requires $\lambda_{irr} < 385$ nm, which disqualifies 95 % of the solar spectrum. In addition, the high recombination rate of the photogenerated species results in a low production rate of secondary photo-generated reactive compounds [4,5]. Diverse approaches such as coupling TiO_2 with other semiconductors [6,7], dye sensitizing [8,9], ion implantation [10], noble metal [4] decoration, doping with heteroatoms [11] now account for several literature data. Among the noble metals Ag NPs have been a target since they also possess antibacterial properties [12]. However, besides this, AgNPs exhibit the surface plasmon band typical of noble metal NPs, which originates from the Mie absorption in the visible spectrum. When incorporated onto TiO_2, its band-gap decreases, opening up the light absorption over a wider light spectrum region. The fundamental mechanism of visible light absorption by TiO_2 decorated with Ag identifies with the injection of metal plasmonic electrons into the wide band-gap semiconductor. However, the plasmonic absorption, which is an optical property at the surface/bulk interface, only manifest for NPs bigger than 2 nm. Below this size, quantum effects prevails [13]. The most recent approaches focus on interposing a layer of conductive material between TiO_2 and Ag to provide a conductive path for the electrons from the noble metal to the TiO_2 surface. For instance, Lang et al. intercalated graphene oxide (GO) nanosheets as bridges between Ag nanocubes and TiO_2 nanosheets to provide a conductive path for the electrons from the plasmonic Ag band to the

semiconductor [14]. Asapu et al. fabricated core-shell super stable Ag-TiO_2-PAH where polyallylaminehydrochloride (PAH) constitute a polycation layer [15], whereas Jbeli et al. Intercalated a chitosan film that formed an AgCl layer between TiO_2 and Ag species [16].

Controlling the dispersion and size of the noble metal over TiO_2 is fundamental to both maximize photocatalytic activity by tackling the mass transfer of active primary and secondary photogenerated species, as well limiting the input of catalyst precursors' and solvents in an approach towards sustainability. For instance, Stucchi et al. doped micrometric (110 nm) TiO_2 with Ag nanoparticles (NPs) in the weight range from 1 to 20 % by means of ultrasound [17]. Zeng et al. synthesized Ag nanowires with TiO_2 NPS around them that were stable for several days and degraded acetaldehyde in few minutes in gas phase under fluorescent light [18].

AgNPs agglomerated electrochemically to control their size is an innovative and interesting approach because it is possible to precisely control the size of Ag. Starowicz et al. polarized a sacrificial anode of Ag and obtained AgNPs of about 20 nm [19]. With the same technique, Rodriguez-Sanchez et al. obtained nanoparticles in the range 2-7 nm in acetonitrile and tetrabutylammonium bromide as electrolyte and stabilizer [19]. TiO_2 particle size is another fundamental issue to tackle the benefits of nanotechnology dominate our thinking nowadays. The concerns regarding nano-particles (< 100 nm) deal with inhalation and skin contact of particles that are so small to be potentially not "recognizable" by the human body barriers, thus reaching the organism cells. The number of papers on the subject "TiO_2 nanoparticles and toxicity", which raised from 57 (within 2008) to 985 in the last 10 years [Scopus.com source], is a proof of the increasing concern about the effects of nano-particles on living beings. Concurrently, major national and international agencies in Europe are promoting research on potential adverse effects of nanoparticles [20]. The effects of nano-sized TiO_2 on human health have not been fully demonstrated yet, but the first data on the adverse effect of nano-sized TiO_2 on animals just became available [21,22].

The authors recently confronted this issue by several papers published on increasing the photoactivity of micro-TiO_2 [23–25], whereby doping micro-sized TiO_2 the activity increased in the visible range.

Among all the pollutants, nitrogen oxides (NOx) are continuously monitored all over the world and guidelines on the alarm levels of these molecules in air were published by WHO [26] and

often recalled in the legislations of single countries worldwide. Photocatalysis with titanium dioxide as a semiconductor seems to be a promising technique to reduce the pollutant concentration due to its powerful oxidation properties. For this reason, the NOx degradation reaction was selected to probe the photocatalytic activity of our samples. Folli et al [27] report a correlation between the maximum NO removal (minimum concentration) with the maximum UV irradiance. Another recent review contribution by Schreck et al. [28] reports about NOx emissions, in particular from the transport sector, as they significantly impact the urban air quality. The band-gap of anatase phase TiO2 is 3.2 eV and the oxidation and reduction potentials of the valance and conduction bands are +2.95 V and −0.25 V, respectively. The reduction potential of NO to N2 is +3.36 V and the oxidation potential of NO to NO3− is −0.934 V indicating that both photooxidation and photoreduction of NO are feasible reactions over TiO_2 [29].

In this paper, we report the electrochemical synthesis of Ag NPs together with their subsequent deposit by incipient wetness on micrometric TiO_2. During the synthesis of the catalyst, the pH was varied in the 4-12 range, observing exceptional catalytic performance (90% NOx conversion in 1 h) under LED light for the sample obtained at pH = 14 and PVP/Ag+ molar ratio = 3.

2. Experimental

2.1 Silver nanoparticles preparation

Ag NPs were prepared from an $AgNO_3$, polyvinyl pyrrolidone (PVP) and KNO_3 solution. KNO_3 (≥ 99.0 %) and PVP (average molecular weight = 40 000) were purchased from Sigma Aldrich and were employed them with no further purification. 100 mL of a 30 g/L $AgNO_3$ solution were placed into a becker containing 1 g of KNO_3 and a weighted amount of PVP. KNO_3 solution was added as supporting electrolyte. PVP acted as physical nanoparticle dispersant [30] and we varied its concentration to gauge the effect of PVP on the synthesis. We varied the dispersant to understand its influence on the stabilization of Ag NPs. We selected polyvinyl alcohol (PVA) (average molecular weight = 9000-10000, 80% hydrolysed, Sigma Aldrich) [31] and polyacrylic acid (PAA, sodium salt, average molecular weight = 8000, Sigma Aldrich) [32]. The counter and working electrode were two platinum foils (40 mm x 20 mm), while the reference electrode was

a saturated calomel electrode (SCE). To protect SCE from AgCl precipitation, we used double bridge filled up with a saturated KNO_3 solution, which acted as second electrolyte.

AUTOLAB potentiostat coupled with Nova software determined the reduction potential for each test through cyclovoltammetry (CV). The cyclic staircase started from 0.4 V, reached a lower potential -0.2 V, increased until 1.0 V, and returned to 0.4 V. The reductive current obtained from CVs was almost constant from + 0.3V to - 0.2V, therefore it was decided to synthetize Ag nanoparticles at +0.2 V, to maximize silver production and to avoid, at the same time, to deposit metallic silver on the electrode. We observed that in this condition, after 10 min, silver only deposited on the working electrode. Therefore, we set the duration of each synthesis to 10 min.

We also modified the pH of the solution after the electrochemical synthesis with either HNO_3 or NH_4OH, to study the influence of pH on the Ag nanoparticles structure/morphology and verify its possible influence of the final photocatalytic performance.

2.2 Catalyst synthesis

During the electrochemical synthesis, the colour of the mixture gradually shifted from white to yellow and became cloudier, thus indicating the formation of nanoparticles. [3].

We then added NH_4OH to the silver nanoparticles (Ag NPs) solution to a pH of 12 to form NH_3. Ammonia stabilizes the dopant in the solution avoiding the formation of Ag_2O precipitate according to Tollens reaction (1-2):

$$2\ AgNO_3 + 2\ OH^- \rightarrow Ag_2O(s) + 2\ NO_3^- + H_2O \quad (1)$$

$$Ag_2O(s) + 4\ NH_3 + 2\ NO_3^- + H_2O \rightarrow 2\ [Ag(NH_3)_2]NO_3 + 2\ OH^- \quad (2)$$

We then suspended TiO_2 (Kronos 1077) in 6 mL of acetone (HPLC grade, Sigma Aldrich). We added the Ag NPs aqueous solution to the suspension to obtain an AgNPs mass loading of 8 % (value optimized in previous works). The solution was kept under stirring for 24 h, at a temperature of 40 °C. After, we raised the temperature to 80 °C for 2 h. At the end of the impregnation, we removed water by evaporation, and heated the mixture to 100 °C. A furnace calcined the powder at 400 °C for 2 h under static atmosphere.

Here we compare 7 catalysts (Table 1) prepared with different conditions. Sample 7 was prepared in the same condition of sample 6 but with 5 times the reagents amount and the volumes (500 mL of $AgNO_3$ solution, 5 g of KNO_3 and 40 cm^2 of working electrode surface) so to verify a possible modification of the final result after a simple scale-up.

Table 1: Synthesis of the Ag-TiO_2 samples.

Sample	Ag NPs loading (% by weight)	mol PVP / mol Ag^+	pH
1	0	-	-
2	8	3:1	12
3	8	50:1	12
4	8	3:1	4
5	8	1:1	4
6	8	1:1	12
7	8	1:1	12

2.3 Characterization

A JEOL 3010–UHR Instrument fitted with a LaB6 filament (acceleration potential 300 kV) and equipped with an Oxford INCA Energy TEM 200 energy dispersive X–ray (EDX) detector (TEM-HRTEM) imaged the samples. Samples were dry dispersed onto Cu grids coated with "lacey" carbon film.

A PANalytical Xpert Multipurpose X-ray Diffractometer measured samples crystallinity. It is equipped with a Cu anode (Kα radiation, λ = 1.54060 nm). The working potential was 45 kV while the working current was 40 mA. We analyzed our samples with a scan rate of 0.05° in a 2θ range of 20°-80°.

An M-Probe (SSI) XPS instrument was used to analyze the samples surfaces detecting in particular Ti_{2p}, O_{1s} and Au_{4f} regions. The instrument is equipped with a monochromatic $Al_{k\alpha}$ anode and is calibrated using C_{1s} at 284.6 eV.

Specific surface area measurements were carried out by conventional N_2 adsorption/desorption (BET) at 77 K by means of a Sorptometer (Costech Mod. 1042) apparatus.

A Thermo Scientific Evolution 600 spectrophotometer equipped with a diffuse reflectance accessory Praying-Mantis sampling kit measured the absorbance, (Harrick Scientific Products, USA). The reference material was a Spectralon1 disk.

2.4 NOx setup

We adopted a 20 L Pyrex glass batch reactor to degrade NOx. The complete description of the setup is reported elsewhere [33] and its scheme is available in the Supporting Information file (S4). We deposited a suspension of (0.050 ±0.001) mg of catalyst in isopropanol (technical grade, Sigma Aldrich) on a glass plate (200 mm x 20 mm). An ultrasonic bath suspended the powder in the alcohol before the deposition. After the evaporation of the solvent, we placed the plate with the catalyst on the top of it inside the reactor. The concentration of the model pollutant was 500 ppb of NOx (initial bottle concentration 0.625 % of NO_2 and 0.125 % of NO, diluted with air). A LED lamp (MW mean well, 350 mA rated current, 9 V to 48 V DC voltage range, 16:8W rated power) with an emission from 400 nm to 700 nm was the photon source set at a distance to have 1000 lux on the sample surface. We set the relative humidity of the reactor at 50 %. Time 0 corresponded to the switching on of the lamp. An Ecotech Serinus 40NOx directly connected to the reactor measured the concentration of both NO and NO_2 at 60, 180 and 360 min.

The calibration of the instrument was verified by sampling directly from the NOx cylinder to the instrument. The concentration of NOx matched the one declared by the gas supplier. The sampling was realized by opening a valve to let the instrument automatically withdraw a gas aliquot from the reactor. The lower detection limit of the instrument is 0.4 ppb and a precision of 0.5 % [34]. Therefore, we calculated the error on the NOx conversion using the formula for the error propagation.

3. Results and discussion

3.1 Selection of the capping agent

The electrochemical synthesis of AgNPs failed with PAA and PVA for different reasons. The carboxylic domains of PAA exchanged sodium ion with silver ion in the solution and formed an insoluble complex that precipitated [35]. PVA did bring to the formation of an AgNPs solution, but that was in turn unstable. For all the concentrations tested, the NPs coagulated and aggregated within 3-4 hours. Literature reports stability for the Ag-PVA complex with increasing dispersant molecular weight and when other rheological additive are present [36]. We filed the synthesis with different concentration of PVA (from 10 to 30 g L^{-1}). We therefore selected PVP for all the synthesis.

3.2 Sample morphology and nanoparticle size distribution

All the samples object of the present research exhibit almost the same value (~ 12 ± 2 m^2 g^{-1}) of BET specific surface area, i.e. the value related to the bare TiO_2 (micrometric sample 1) despite the presence of Ag NPS.

TEM confirmed that the average dimensions for sample 1 (i.e., bare Kronos 1077) are around 110 nm. Its particles are well ordered, in most cases they are thin and not too much closed packed together. A detailed inspection at higher magnification (see Supporting Information Fig S1) indicates that all the particles are highly crystalline: the calculated distances (0.35_2 nm) among the fringes evidence that the most frequently exposed crystal planes belong to the (101) family of anatase [ICDD 21-1272]. This feature is also confirmed by the analysis of the electron diffraction.

The general morphology of the supporting material remains unchanged for Sample 2, despite the procedure followed to add silver species. Sample 2 exhibits the same external habit of the titania crystals reported for sample 1 and the same fringe patterns ascribable to anatase (see Figure 2b).

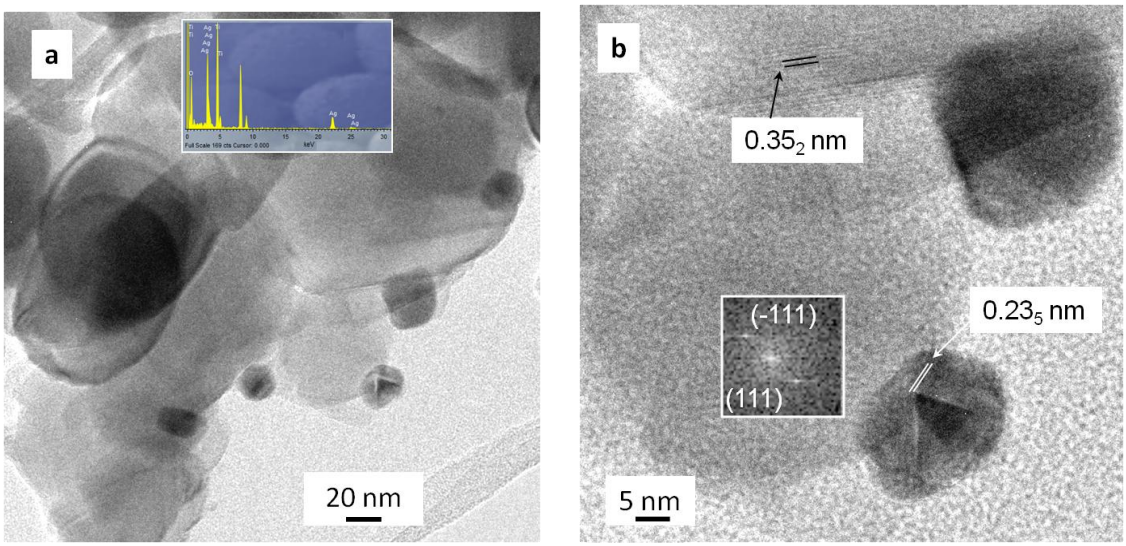

Figure 2. C-TEM (section a) and HR-TEM (section b) images referred to sample 2.

The extra particles present in Figure 2a, characterized by a much lower size and higher contrast as well, are made up of Ag. This is confirmed by different experimental evidences: (i) the EDX analysis, reported in the inset to Figure 2a, indicates the presence of metallic Ag, besides Ti and O; (ii) the inspection of the fringe patterns exhibited by the smaller particles (Figure 2b) puts into evidence that the calculated 0.23 nm distances are ascribable to metallic silver [ICDD 004-0783]. Sample 3 resembles sample 2 (Figure 3). Both samples have been synthesized in similar pH (basic) conditions but with different PVP.

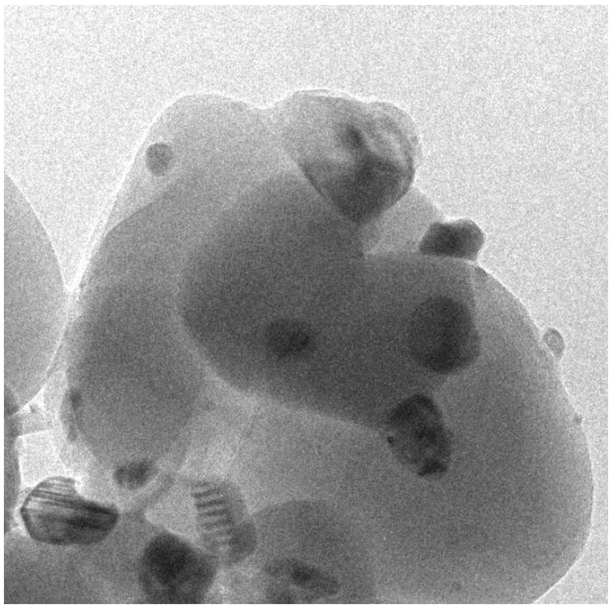

Figure 3. C-TEM image referred to sample 3

Samples 4 and 5 were synthetized in acidic conditions. Their morphology confirms to be unaltered for the titania support, but deeply different for what concerns the Ag NPs appearance (see Figure 4 and 5, respectively). In fact, their size is much smaller, being far beyond a half than in the case of the samples obtained at basic pH.

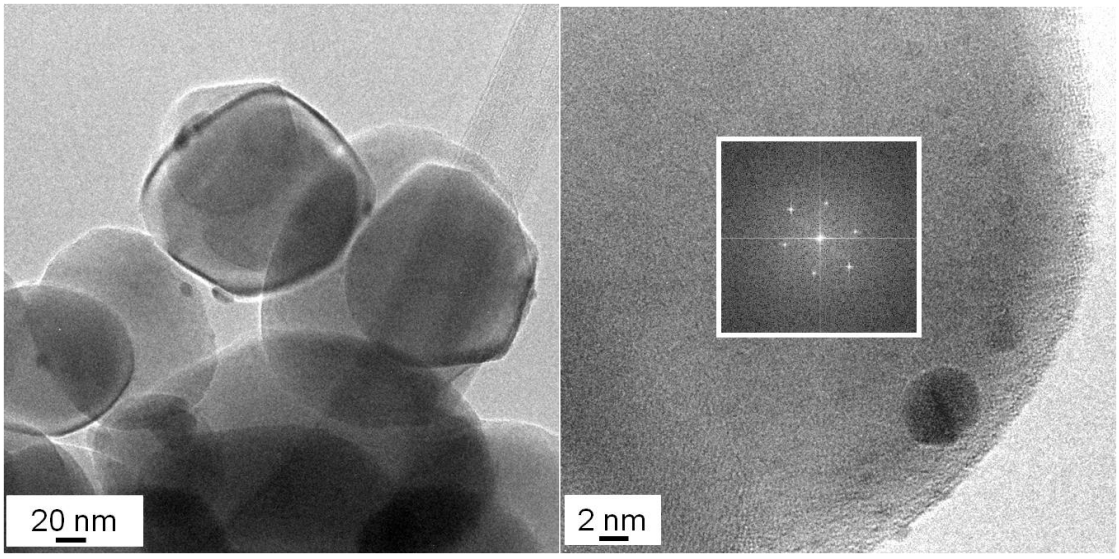

Figure 4. C-TEM (section a) and HR-TEM (section b) images referred to sample 4.

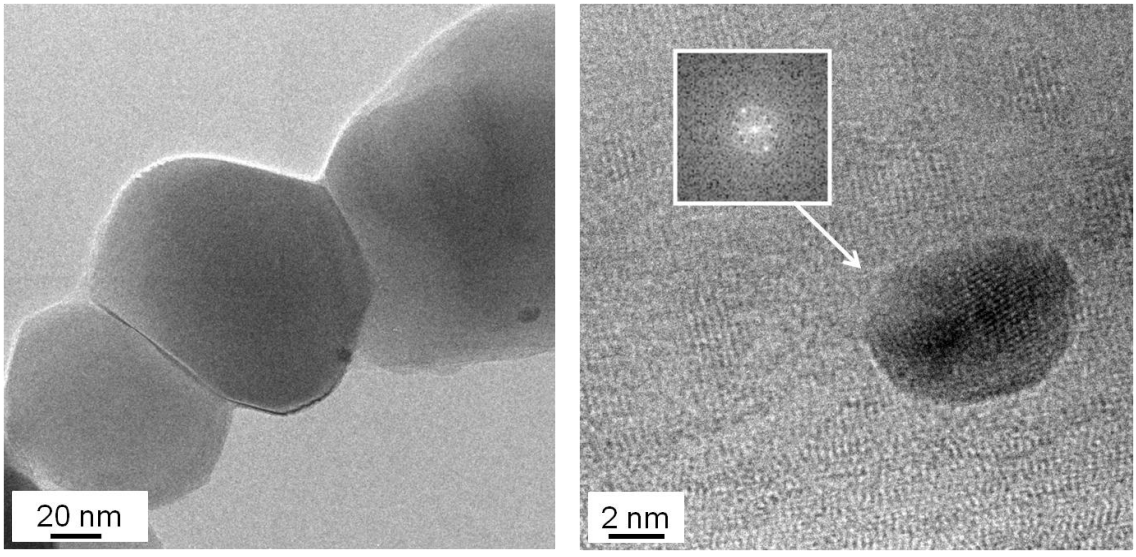

Figure 5. C-TEM (section a) and HR-TEM (section b) images referred to sample 5.

In the case of sample 6 the situation is intermediate between the two above described: see Figure 6. Sample 7 shows the same morphology of sample 6 confirming that the scale-up process does not alter the AgNPs features.

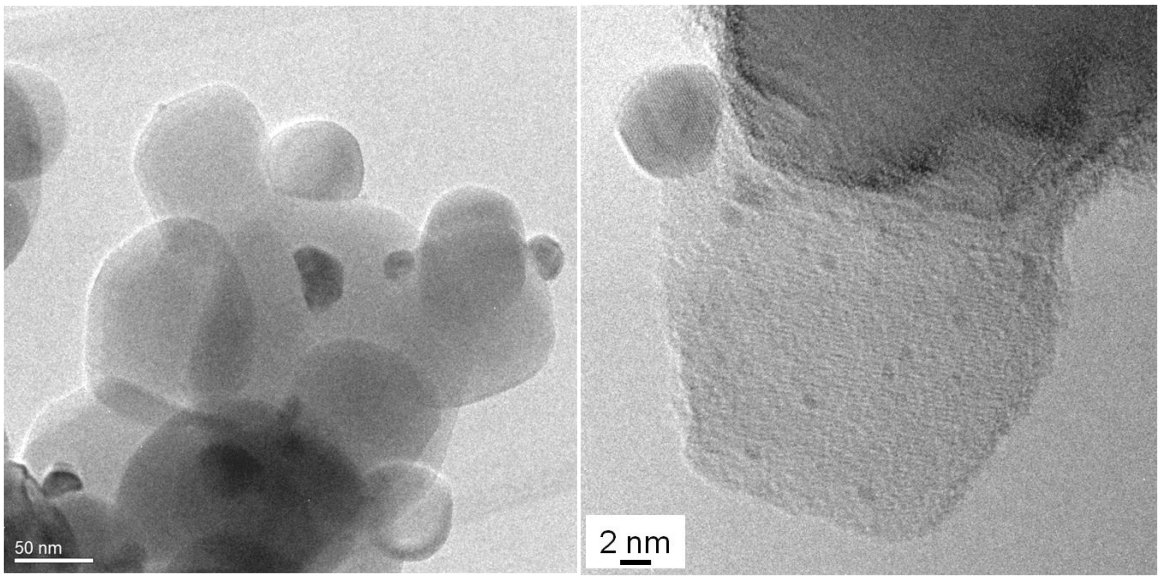

Figure 6. C-TEM (section a) and HR-TEM (section b) images referred to sample 6.

For samples 2, 3 and 6 (and 7) there is a broader spread of Ag NPs dimensions, ranging in the 5-25 nm (with dominating dimensions in the 15-20 nm range, Supporting Information Figure S2) with respect to samples 4 and 5, for which the distribution is much narrower and whose mean size is located in the 1-5 nm range.

The amount of silver in the various preparations (Table 1) was constant ($8\%_{wt}$), whereas the parameters that have been changed are either the amount of the PVP dispersing agent or the pH of the solutions before the electrochemical synthesis.

In the condition of constant pH (no matter acidic or basic), the effect of a different amount of PVP is almost negligible, as the relevant AgNPs distribution are similar for the two pH values. Our results hold also considering diverse AgNPs preparation methods. Malina et al. [37] reduced

$AgNO_3$ with $NaBH_4$ varying the concentration of PVP. They did not see a significant change in AgNPs size below a concentration of 10 % of PVP. Moreover, changing PVP concentration leads to similar NPs distribution during the laser ablation preparation method [38].

On the other hand, the different pH values have a great influence in the Ag NPs distributions. In fact, changing pH from 11.5 to 12.5 leads to bigger nanoparticles when the reducing agent is a sugar [39]. Therefore, pH possesses a leading role in determining the ultimate size(s) of the AgNPs, during the direct electrochemical reduction of $AgNO_3$.

The crystallographic phase composition of the various samples has been assessed also based on the X-Ray diffraction investigation: Figure 7 summarizes the relevant results for the 2 to 5 powders.

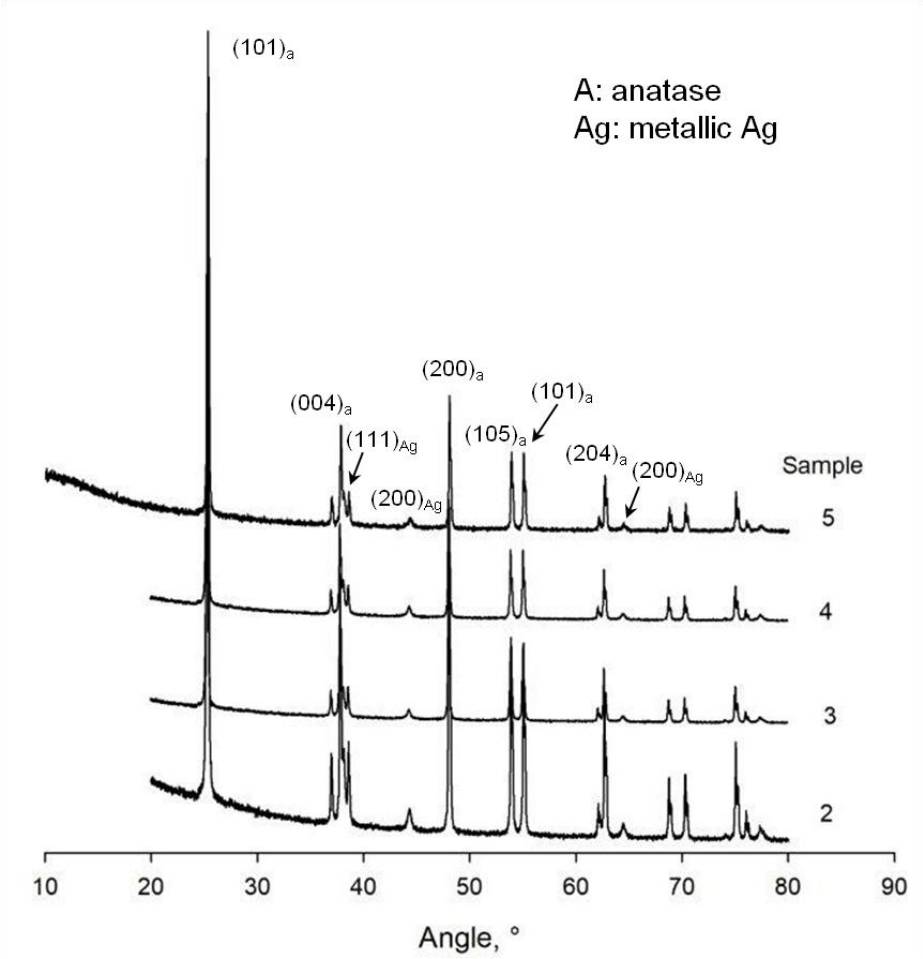

Figure 7: XRD of samples 2-5.

It is well evident that the main features are ascribable to the anatase TiO_2 polymorph, as expected also on the basis of the morphological characterization carried out by means of HR-

TEM investigation. In all the diffractograms, the main peak at 2θ ~ 25° can be ascribed to the most intense (101) peak due to anatase [ICDD card n. 21-1272], as well as many other reflexes: a few differences in intensity for the minor peaks is observable, but this is the only peculiarity that can be evidenced in particular for sample 4 and 5, synthesized in acidic conditions. Besides these peaks, a clear indication of the presence of metallic Ag comes from the three reflexes located at 2θ ~ 38°, 44 ° and 65°, respectively ascribable to (111), (200) and (200) crystal planes [on the basis of metallic Ag ICDD card n. 4-0783]. No extra peaks are observable that can indicate the presence of oxidated Ag species: this fact may be due to the very low amount of these species (if present most likely due to passivation effects), lying then under the detection power of the XRD technique. For this reason, we resorted the XPS analysis in order to shed some light onto this feature.

High-resolution XPS for O 1s region (sample 6) is the sum of three contributions: a main peak centred at 530 eV, representing the lattice oxygen of TiO_2, a less intense shoulder peak with binding energy at 531 eV, corresponding to the lattice oxygen of Ag_xO, and a third shoulder peak at 532 eV, related to OH species [40] (Fig. 8 right).

Ti 2p spectrum (Supporting Information, Figure S3) only highlights the presence of a single doublet typical of Ti^{4+} in TiO_2.

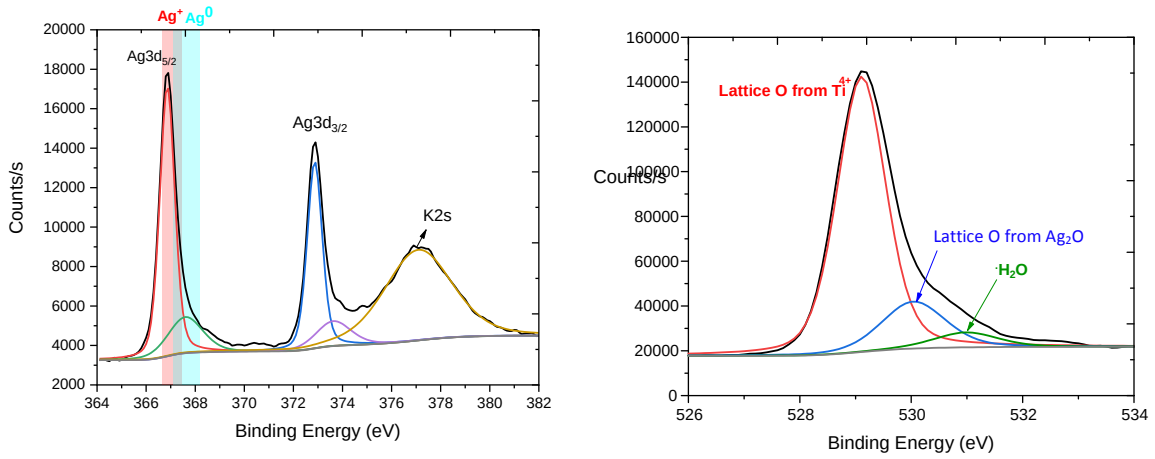

Figure 8: XPS High-resolution spectrum of O1s (right) and Ag3d (left) for sample 6

The ratio between the areas of the peaks located at 529 and 532 eV, respectively, gives useful information about the hydroxyl species (OH) located at the surface of the photocatalyst. In particular, if we compare the OH/O_{tot} ratio calculated for samples 6 and 1 (bare TiO_2), we obtain 0.06 and 0.32 [36], respectively: on the basis of this evidence, we can preliminary conclude sample 6 activity is related to the creation of oxyradicals in situ, favoured because of controlled humidity (50 %) (see the NOx degradation section).

The Ag3d XPS spectrum of sample 6 (Figure 8 left) fits into two separated peaks, one referring to Ag^0 and the other one to its higher valence state Ag^+/Ag_xO [35]. The presence of higher valence state Ag confirms the deduction made discussing the O1s XPS spectrum, due to the presence of a fitted peak at ~531 eV. Due to the calcination in air during the final preparation step, a mix of metal and oxidized Ag nanoparticles are present on the surface of the TiO_2 micro-particles. This morphological feature has not been evidenced by the HR-TEM inspection, as the fraction of oxidized AgNPs is most likely so low that lies under the detection power of this experimental technique.

A modification of the UV-Vis spectra is also evident (supporting information, Figure S5) with an increase of the adsorption at wavelengths in the visible range of 400 nm and 700 nm for all samples but mainly for sample 6.

3.3 NOx degradation

Bare 1077 micro TiO_2 (sample 1) is ineffective towards NOx degradation under visible light. Our result is comparable to the literature and confirms that this material is only active under UV light [33].

Sample 2 exhibits exceptional activity. It converts 90 % of NOx after 1 h of irradiation. Sample 3, 5 and 6 have similar kinetics, while sample 4 is the least active among the series (Figure 9 a). Sample 7 shows the same result of sample 6 even if it was prepared with 5 times the volumes of reagents. Therefore, the properties of this catalyst is unaffected by the volume of the synthesis.

All the catalysts tend to deactivate after 6 h due to the reaction mechanism that brings to the formation of nitrate species (NO_3^-), which we already detected in previous works employing photocatalytic tiles [33,41].

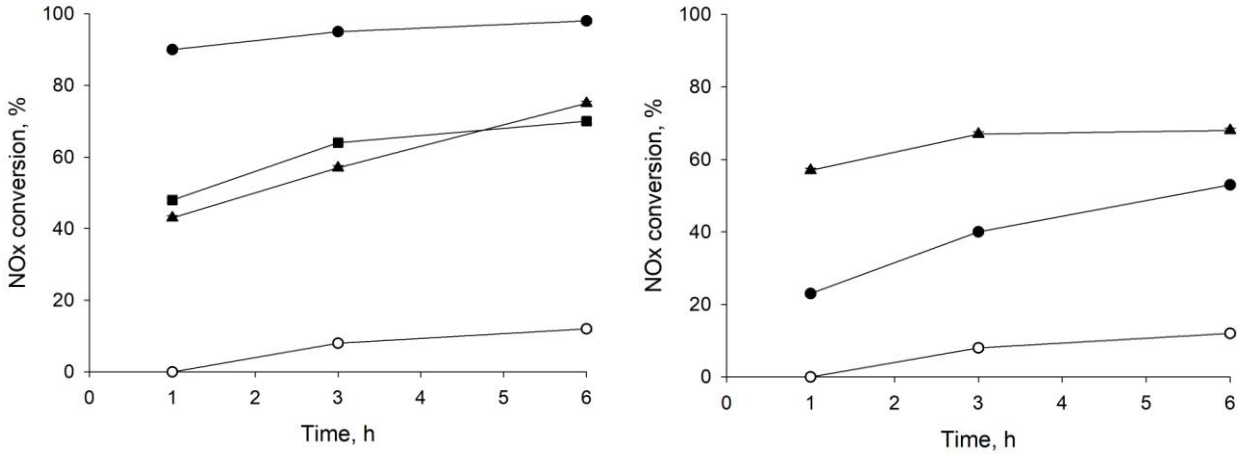

Figure 9 : NOx conversion versus time for catalysts prepared at basic (left side) and acid (right side) pH. Empty symbols correspond to Kronos 1077 while triangles, points and squares represent a PVP/Ag molar ratio of 1, 3 and 50, respectively.

Ag NPs, as well as gold NPs, degrade VOC through different mechanisms depending on the light source and their morphology [42]. Here, we adopted LED light, whose energy is insufficient to directly promote electrons to the valance band of TiO_2. Therefore, localized surface plasmon resonance (LSPR) absorption in Ag NPs is the main effect that makes our samples active. However, when nanoparticles cluster, the absorption is broader and covers a wavelength range of 350 – 500, a range that falls in the emission of the LED lamp employed in our study, which also contribute to their activity, even if to a lower extent.

The optimal PVP/Ag+ molar ratio at pH = 4 was 1, while at pH = 12 it becomes 3 (Figure 10). We hypothesize that this is connected to the particle dimensions. At acid pH, smaller particles form (1-5 nm), therefore less PVP is needed to stabilize them, even though their number is higher, and as a matter of fact, an AgNP size smaller than 5 nm leads to lower NOx conversions.

Sarina et al. correlated the conversion of a photocatalytic reaction (ethylene oxidation) to the plasmon intensity [42]. In another work, Amendola et al. calculated the LSPR of different AgNPs, varying their shapes and assemblies [43]. A single spherical AgNP (radius = 10 nm) absorbs light whose wavelength is between 350 and 450 nm. The same authors also demonstrated that AgNPs smaller than 5 nm, like the ones we obtained in the synthesis with pH

= 4, broaden the absorption band, which correlates with their lower performances compared to catalyst prepared at basic pH.

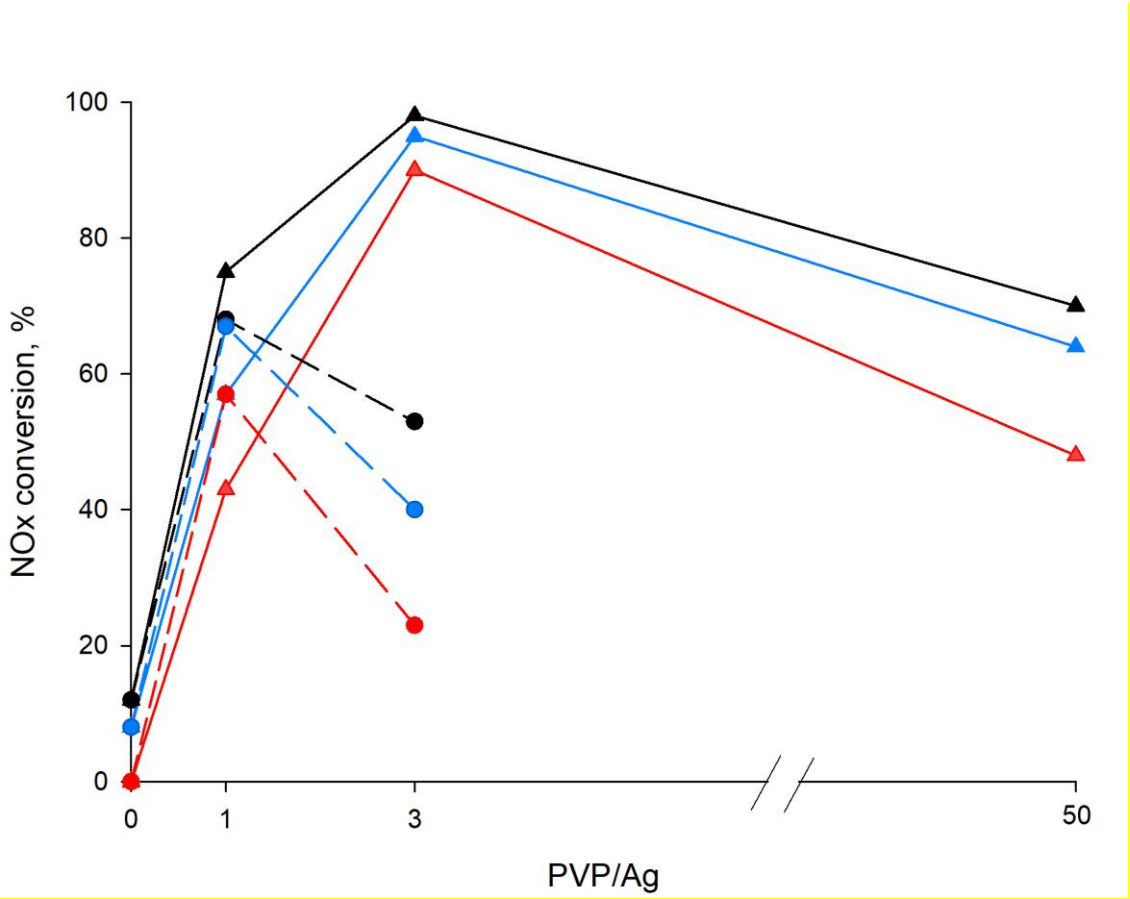

Figure 10: PVP/Ag molar ratio versus NOx conversion for acid pH (dotted lines and points) and basic pH (full line and triangles). Red, blue and black lines represent conversion at time 1 h, 3 h, and 6 h, respectively.

4. Conclusion

In the present contribution we synthetized AgNPs reducing silver nitrate in solution by an electrochemical method. The pH of the solution tailors the dimension of the nanoparticles. At pH = 4 we obtained a NPs distribution 1-5 nm, whereas at pH = 12 this figure becomes 5-25 nm. pH

and polyvinyl pyrrolidone has no influence on the crystallinity of samples and the calcination procedure we propose (400 °C for 2 h in air) yield stable nanoparticles.

As for the titania photocatalyst support, we decided to employ a micrometric commercial system (1077 by Kronos) rather than a nanometric powder, in order to avoid all the possible drawbacks typical of the interaction of NPs with human tissues by either inhalation or skin contact. The photocatalysts we obtained retain all the positive properties due to the micrometric support, such as SSA, crystallographic phase composition, being thus positively influenced in their photocatalytic performances by the promotion by AgNPs, even though a different photodegradation behaviour, as a function of the different AgNPs preparation route, has been put into evidence.

In particular, photocatalytic degradation of NOx under LED light evidenced that the samples prepared at basic conditions exhibit better performances rather than those prepared at acid conditions: AgNPs with diameters of 1-5 nm are less active under LED light because of the broadening of the surface plasmon band. Moreover, the synthesis was scaled up to 500 mL volume, without affecting the final catalysts performances.

Acknowledgements

The Authors acknowledge Projet de cooperation Quebec Italie 2017-2019 (project number: QU17MO09) for granting the mobility of researchers between Canada and Italy. This research was undertaken, in part, thanks to funding from the Canada Research Chairs program.

References

[1] G. Mamba, J. Kiwi, C. Pulgarin, R. Sanjines, S. Giannakis, S. Rtimi, Evidence for the degradation of an emerging pollutant by a mechanism involving iso-energetic charge transfer under visible light, Appl. Catal. B Environ. 233 (2018) 175–183. doi:10.1016/j.apcatb.2018.03.109.

[2] C. Pirola, D.C. Boffito, S. Vitali, C.L. Bianchi, Photocatalytic coatings for building industry: study of 1 year of activity in the NO x degradation, J. Coatings Technol. Res. 9 (2012) 453–458. doi:10.1007/s11998-011-9381-7.

[3] M. Hosseini-Sarvari, F. Jafari, A. Mohajeri, N. Hassani, Cu 2 O/TiO 2 nanoparticles as visible light photocatalysts concerning C(sp 2)–P bond formation, Catal. Sci. Technol. 8 (2018) 4044–4051. doi:10.1039/C8CY00822A.

[4] Z. Wei, M. Janczarek, M. Endo, K. Wang, A. Balčytis, A. Nitta, M.G. Méndez-Medrano, C. Colbeau-Justin, S. Juodkazis, B. Ohtani, E. Kowalska, Noble metal-modified faceted anatase titania photocatalysts: Octahedron versus decahedron, Appl. Catal. B Environ. 237 (2018) 574–587. doi:10.1016/j.apcatb.2018.06.027.

[5] Z. Song, B. Hong, X. Zhu, F. Zhang, S. Li, J. Ding, X. Jiang, J. Bao, C. Gao, S. Sun, CdS/Au/Ti/Pb(Mg1/3Nb2/3)0.7Ti0.3O3 photocatalysts and biphotoelectrodes with ferroelectric polarization in single domain for efficient water splitting, Appl. Catal. B Environ. 238 (2018) 248–254. doi:https://doi.org/10.1016/j.apcatb.2018.07.033.

[6] N. Saadatkhah, M.G. Rigamonti, D.C. Boffito, H. Li, G.S. Patience, Spray dried SiO 2 WO 3 /TiO 2 and SiO 2 vanadium pyrophosphate core-shell catalysts, Powder Technol. 316 (2017) 434–440. doi:10.1016/j.powtec.2016.10.056.

[7] H. Khan, M.G. Rigamonti, G.S. Patience, D.C. Boffito, Spray dried TiO 2 /WO 3 heterostructure for photocatalytic applications with residual activity in the dark, Appl. Catal. B Environ. 226 (2018) 311–323. doi:10.1016/j.apcatb.2017.12.049.

[8] Z. Wang, X. Lang, Visible light photocatalysis of dye-sensitized TiO2: The selective aerobic oxidation of amines to imines, Appl. Catal. B Environ. 224 (2018) 404–409. doi:10.1016/j.apcatb.2017.10.002.

[9] X. Li, J.-L. Shi, H. Hao, X. Lang, Visible light-induced selective oxidation of alcohols with air by dye-sensitized TiO 2 photocatalysis, Appl. Catal. B Environ. 232 (2018) 260–267. doi:10.1016/j.apcatb.2018.03.043.

[10] A. Utsunomiya, A. Okemoto, Y. Nishino, K. Kitagawa, H. Kobayashi, K. Taniya, Y. Ichihashi, S. Nishiyama, Mechanistic study of reaction mechanism on ammonia photodecomposition over Ni/TiO 2 photocatalysts, Appl. Catal. B Environ. 206 (2017) 378–383. doi:10.1016/j.apcatb.2017.01.045.

[11] I. Milošević, S. Rtimi, A. Jayaprakash, B. van Driel, B. Greenwood, A. Aimable, M.

Senna, P. Bowen, Synthesis and characterization of fluorinated anatase nanoparticles and subsequent N-doping for efficient visible light activated photocatalysis, Colloids Surfaces B Biointerfaces. 171 (2018) 445–450. doi:10.1016/j.colsurfb.2018.07.035.

[12] S. Rtimi, D.D. Dionysiou, S.C. Pillai, J. Kiwi, Advances in catalytic/photocatalytic bacterial inactivation by nano Ag and Cu coated surfaces and medical devices, Appl. Catal. B Environ. 240 (2019) 291–318. doi:10.1016/j.apcatb.2018.07.025.

[13] A. Moores, F. Goettmann, The plasmon band in noble metal nanoparticles: an introduction to theory and applications, New J. Chem. 30 (2006) 1121. doi:10.1039/b604038c.

[14] Q. Lang, Y. Chen, T. Huang, L. Yang, S. Zhong, L. Wu, J. Chen, S. Bai, Graphene "bridge" in transferring hot electrons from plasmonic Ag nanocubes to TiO2 nanosheets for enhanced visible light photocatalytic hydrogen evolution, Appl. Catal. B Environ. 220 (2018) 182–190. doi:10.1016/j.apcatb.2017.08.045.

[15] R. Asapu, N. Claes, S. Bals, S. Denys, C. Detavernier, S. Lenaerts, S.W. Verbruggen, Silver-polymer core-shell nanoparticles for ultrastable plasmon-enhanced photocatalysis, Appl. Catal. B Environ. 200 (2017) 31–38. doi:10.1016/j.apcatb.2016.06.062.

[16] A. Jbeli, Z. Hamden, S. Bouattour, A.M. Ferraria, D.S. Conceição, L.F.V. Ferreira, M.M. Chehimi, A.M.B. do Rego, M. Rei Vilar, S. Boufi, Chitosan-Ag-TiO2 films: An effective photocatalyst under visible light, Carbohydr. Polym. 199 (2018) 31–40. doi:10.1016/j.carbpol.2018.06.122.

[17] M. Stucchi, C.L. Bianchi, C. Argirusis, V. Pifferi, B. Neppolian, G. Cerrato, D.C. Boffito, Ultrasound assisted synthesis of Ag-decorated TiO2 active in visible light, Ultrason. Sonochem. 40 (2018) 282–288. doi:10.1016/j.ultsonch.2017.07.016.

[18] Q. Zeng, X. Xie, X. Wang, Y. Wang, G. Lu, D.Y.H. Pui, J. Sun, Enhanced photocatalytic performance of Ag@TiO2 for the gaseous acetaldehyde photodegradation under fluorescent lamp, Chem. Eng. J. 341 (2018) 83–92. doi:10.1016/j.cej.2018.02.015.

[19] M. Starowicz, B. Stypuła, J. Banaś, Electrochemical synthesis of silver nanoparticles, Electrochem. Commun. 8 (2006) 227–230. doi:10.1016/j.elecom.2005.11.018.

[20] K. Ozawa, M. Emori, S. Yamamoto, R. Yukawa, S. Yamamoto, R. Hobara, K. Fujikawa,

H. Sakama, I. Matsuda, Electron–Hole Recombination Time at TiO 2 Single-Crystal Surfaces: Influence of Surface Band Bending, J. Phys. Chem. Lett. 5 (2014) 1953–1957. doi:10.1021/jz500770c.

[21] F. Hong, L. Wang, Nanosized titanium dioxide-induced premature ovarian failure is associated with abnormalities in serum parameters in female mice, Int. J. Nanomedicine. Volume 13 (2018) 2543–2549. doi:10.2147/IJN.S151215.

[22] P. Sá-Pereira, M.S. Diniz, L. Moita, T. Pinheiro, E. Mendonça, S.M. Paixão, A. Picado, Protein profiling as early detection biomarkers for TiO2 nanoparticle toxicity in Daphnia magna, Ecotoxicology. 27 (2018) 430–439. doi:10.1007/s10646-018-1907-7.

[23] M. Stucchi, D. Boffito, E. Pargoletti, G. Cerrato, C. Bianchi, G. Cappelletti, Nano-MnO2 Decoration of TiO2 Microparticles to Promote Gaseous Ethanol Visible Photoremoval, Nanomaterials. 8 (2018) 686. doi:10.3390/nano8090686.

[24] G. Cerrato, C.L. Bianchi, F. Galli, C. Pirola, S. Morandi, V. Capucci, Micro-TiO2 coated glass surfaces safely abate drugs in surface water, J. Hazard. Mater. 363 (2019) 328–334. doi:10.1016/j.jhazmat.2018.09.057.

[25] M. Stucchi, C.L. Bianchi, C. Pirola, S. Vitali, G. Cerrato, S. Morandi, C. Argirusis, G. Sourkouni, P.M. Sakkas, V. Capucci, Surface decoration of commercial micro-sized TiO2 by means of high energy ultrasound: A way to enhance its photocatalytic activity under visible light, Appl. Catal. B Environ. 178 (2015) 124–132. doi:10.1016/j.apcatb.2014.10.004.

[26] WHO, Ambient (outdoor) air quality and health, (2018). https://www.who.int/news-room/fact-sheets/detail/ambient-(outdoor)-air-quality-and-health (accessed February 1, 2019).

[27] A. Folli, J.Z. Bloh, M. Strøm, T. Pilegaard Madsen, T. Henriksen, D.E. Macphee, Efficiency of Solar-Light-Driven TiO 2 Photocatalysis at Different Latitudes and Seasons. Where and When Does TiO 2 Really Work?, J. Phys. Chem. Lett. 5 (2014) 830–832. doi:10.1021/jz402704n.

[28] M. Schreck, M. Niederberger, Photocatalytic Gas Phase Reactions, Chem. Mater. (2019)

acs.chemmater.8b04444. doi:10.1021/acs.chemmater.8b04444.

[29] N. Bowering, G.S. Walker, P.G. Harrison, Photocatalytic decomposition and reduction reactions of nitric oxide over Degussa P25, Appl. Catal. B Environ. 62 (2006) 208–216. doi:10.1016/j.apcatb.2005.07.014.

[30] B. Yin, H. Ma, S. Wang, S. Chen, Electrochemical Synthesis of Silver Nanoparticles under Protection of Poly(N -vinylpyrrolidone), J. Phys. Chem. B. 107 (2003) 8898–8904. doi:10.1021/jp0349031.

[31] R. Surudzic, Z. Jovanovic, N. Bibic, B. Nikolic, V. Miskovic-Stankovic, Electrochemical synthesis of silver nanoparticles in poly(vinyl alcohol) solution, J. Serbian Chem. Soc. 78 (2013) 2087–2098. doi:10.2298/JSC131017124S.

[32] S. Magdassi, M. Grouchko, O. Berezin, A. Kamyshny, Triggering the Sintering of Silver Nanoparticles at Room Temperature, ACS Nano. 4 (2010) 1943–1948. doi:10.1021/nn901868t.

[33] C.L. Bianchi, C. Pirola, F. Galli, G. Cerrato, S. Morandi, V. Capucci, Pigmentary TiO2: A challenge for its use as photocatalyst in NOx air purification, Chem. Eng. J. 261 (2015) 76–82. doi:10.1016/j.cej.2014.03.078.

[34] Ecotech, Serinus 40 brochure, (2018) 2. https://www.ecotech.com/wp-content/uploads/2015/03/ECOTECH-Serinus-40-NOx-Gas-Analyser-spec-sheet-20181202.pdf (accessed January 21, 2019).

[35] J.A. Dean, Lange's Handbook Of Chemistry, 15th ed., 1999.

[36] K.A. Juby, C. Dwivedi, M. Kumar, S. Kota, H.S. Misra, P.N. Bajaj, Silver nanoparticle-loaded PVA/gum acacia hydrogel: Synthesis, characterization and antibacterial study, Carbohydr. Polym. 89 (2012) 906–913. doi:10.1016/j.carbpol.2012.04.033.

[37] D. Malina, A. Sobczak-Kupiec, Z. Wzorek, Z. Kowalski, Silver nanoparticles synthesis with different concentrations of Polyvinylpyrrolidone, Dig. J. Nanomater. Biostructures. 7 (2012) 1527–1534.

[38] T. Tsuji, D.-H. Thang, Y. Okazaki, M. Nakanishi, Y. Tsuboi, M. Tsuji, Preparation of

silver nanoparticles by laser ablation in polyvinylpyrrolidone solutions, Appl. Surf. Sci. 254 (2008) 5224–5230. doi:10.1016/j.apsusc.2008.02.048.

[39] A. Panáček, L. Kvítek, R. Prucek, M. Kolář, R. Večeřová, N. Pizúrová, V.K. Sharma, T. Nevěčná, R. Zbořil, Silver Colloid Nanoparticles: Synthesis, Characterization, and Their Antibacterial Activity, J. Phys. Chem. B. 110 (2006) 16248–16253. doi:10.1021/jp063826h.

[40] H. Ren, P. Koshy, F. Cao, C.C. Sorrell, Multivalence Charge Transfer in Doped and Codoped Photocatalytic TiO 2, Inorg. Chem. 55 (2016) 8071–8081. doi:10.1021/acs.inorgchem.6b01200.

[41] C.L. Bianchi, C. Pirola, F. Galli, S. Vitali, A. Minguzzi, M. Stucchi, F. Manenti, V. Capucci, NO x degradation in a continuous large-scale reactor using full-size industrial photocatalytic tiles, Catal. Sci. Technol. 6 (2016) 2261–2267. doi:10.1039/C5CY01627D.

[42] S. Sarina, E.R. Waclawik, H. Zhu, Photocatalysis on supported gold and silver nanoparticles under ultraviolet and visible light irradiation, Green Chem. 15 (2013) 1814. doi:10.1039/c3gc40450a.

[43] V. Amendola, O.M. Bakr, F. Stellacci, A Study of the Surface Plasmon Resonance of Silver Nanoparticles by the Discrete Dipole Approximation Method: Effect of Shape, Size, Structure, and Assembly, Plasmonics. 5 (2010) 85–97. doi:10.1007/s11468-009-9120-4.